Tripathy, Ratna and Kunwar, Prabhat S. and Sano, Hiroko and Renault, Andrew D. (2014) Transcriptional regulation of Drosophila gonad formation. Developmental Biology, 392 (2). pp. 193-208. ISSN 0012-1606

Transcriptional regulation of *Drosophila* gonad formation

Ratna Tripathy, Prabhat S. Kunwar[1,3], Hiroko Sano[2,3] and Andrew D. Renault[4]*

Max Planck Institute for Developmental Biology, Spemannstr. 35, 72074 Tübingen, Germany

[1]Division of Biology, California Institute of Technology, Pasadena, California, United States of America

[2]Department of Molecular Genetics, Institute of Life Sciences, Kurume University, Kurume, Fukuoka, Japan

[3]equal contribution

[4]current address: School of Life Sciences, Nottingham University, Queen's Medical Centre, Nottingham, NG7 2UH

*corresponding author

Phone: +44 115 82 30505

E-mail: andrew.renault@nottingham.ac.uk

Abstract

The formation of the *Drosophila* embryonic gonad, involving the fusion of clusters of somatic gonadal precursor cells (SGPs) and their ensheathment of germ cells, provides a simple and genetically tractable model for the interplay between cells during organ formation. In a screen for mutants affecting gonad formation we identified a SGP cell autonomous role for Midline (Mid) and Longitudinals lacking (Lola). These transcriptional factors are required for multiple aspects of SGP behaviour including SGP cluster fusion, germ cell ensheathment and gonad compaction.

The *lola* locus encodes more than 25 differentially spliced isoforms and we have identified an isoform specific requirement for *lola* in the gonad which is distinct from that in nervous system development. Mid and Lola work in parallel in gonad formation and surprisingly Mid overexpression in a *lola* background leads to additional SGPs at the expense of fat body cells. Our findings support the idea that although the transcription factors required by SGPs can ostensibly be assigned to those being required for either SGP specification or behaviour, they can also interact to impinge on both processes.

Keywords

germ cell; somatic gonadal precursor; Drosophila; midline; longitudinals lacking; gonad; tinman

Introduction

To generate intricate tissues and organs from more homogeneous cell populations during development, cells must work together. Whilst the number of cell types involved and the final patterns are diverse for different organs, the underlying rationale is broadly similar, involving changes in cell shape, position, adhesive and junctional properties and the development of specialized cellular activities, such as secretion or contraction. How these processes are initiated and coordinated at a molecular level are largely unknown.

The *Drosophila* gonad at the end of embryogenesis has a ball-like conformation of just two interspersed cell types and is therefore a good model to understand how cells can cooperate to generate a relatively simple structure. The two cell types of the gonad are the germ cells, which will give rise to sperm and eggs in the adult, and somatic cells termed the somatic gonadal precursors (SGPs) that will create a niche to provide survival signals to the germ cells, and produce supporting cell lineages. The germ cells and SGPs are specified at different embryonic positions and therefore the germ cells migrate to find and associate with the SGPs in order to form the gonad (Richardson and Lehmann, 2010).

The SGPs are specified bilaterally in the mesoderm at embryonic stage 11 as three separate clusters (Brookman et al., 1992). A fourth 'male-specific' SGP (msSGP) cluster is also specified in both sexes, but is maintained only in males (DeFalco et al., 2003). SGP specification requires the activity of a number of homeobox-containing transcription factors including *tinman* (*tin*), *zinc finger homeodomain-1* (*zfh-1*), *abdominal-A* (*abd-A*) and *Abdominal-B* (*Abd-B*) (Broihier et al., 1998). Indeed mis-expression of *abd-A* or *zfh-1* generates ectopic SGPs indicating the instructive nature of at least some of these genes for SGP specification (Boyle and DiNardo, 1995; Broihier et al., 1998; Greig and Akam, 1995).

Other transcription factors are required to maintain SGP fate. For example in *eyes absent* (*eya)*, also known as *clift* (*cli*), mutants, the SGPs are lost soon after they are specified. However, unlike *abd-A*, *eya* mis-expression is not sufficient to induce additional SGPs (Boyle et al., 1997).

Following specification, some of the SGP clusters will encounter migrating

germ cells upon entry of germ cells into the mesoderm at stage 11. The germ cells remain loosely associated with the SGPs until stage 13. At this point the three SGP clusters fuse to form an elongated gonad and the SGPs extend cytoplasmic processes to surround and individualize the germ cells in a process called 'ensheathment' (Boyle and DiNardo, 1995) (see also Figure 2A). Subsequently, the gonads round up in the so called 'compaction' step, and by stage 15 the embryonic gonad appears as a tight ball-like structure.

A number of proteins have been identified as being required to implement the SGP ensheathment and compaction program. Many of these go on to regulate the cell adhesion molecule DE-cadherin (encoded by *shotgun*, *shg*). DE-cadherin is expressed by germ cells and SGPs and is required for ensheathment and compaction (Jenkins et al., 2003). DE-cadherin is downstream of *eya* and is post transcriptionally regulated by two other genes required for gonad formation, *fear of intimacy* (*foi*), which encodes a zinc ion transporter (Mathews et al., 2006) and *enabled* (*ena*) which encodes an actin regulator (Sano et al., 2012). The transcription factor, Traffic Jam (Tj) is required for SGP ensheathment and although it negatively regulates DE-cadherin expression in the adult ovary (Li et al., 2003), how it functions during embryogenesis is not known.

raw mutants also show SGP ensheathment defects (Weyers et al., 2011). Although the molecular function of Raw is not known, it acts by also affecting a cell adhesion molecule, in this case Armadillo (Arm) (Jemc et al., 2012). A critical role for the ligand-receptor pair Slit and Roundabout (Robo) was recently reported, but a permissive rather than directionally instructive role on SGP behaviour was suggested (Weyers et al., 2011).

In a screen for mutants affecting germ cell migration we identified a role for the transcription factors Midine (Mid) and Longitudinals lacking (Lola) in gonad formation. In *mid* and *lola* mutants, SGP cluster fusion, germ cell ensheathment and gonad compaction are perturbed. In this work we explore the isoform specific requirements of Lola in both gonad and nervous system development and define the regulatory relationship between Mid and Lola and with respect to other genes either important for SGPs or linked to Mid in other tissues.

Methods

Fly stocks

The following *Drosophila* lines were from the Bloomington stock center: *Df(2R)ED2098, Df(2R)BSC336, lola[e76]* (Madden et al., 1999), *mid[1], mid[2]* (Liu et al., 2009; Nusslein-Volhard et al., 1984), *UASlola-B* (Spletter et al., 2007), *nosGal4VP16* (Van Doren et al., 1998), and *PBac{lola.GR-GFP.FLAG}VK00033. lola[22.05]* was a gift from Mark Van Doren (Weyers et al., 2011), *UASmid* (Buescher et al., 2004) and *mid4.3>lacZ* (Ryu et al., 2011) was a gift of William Brook. The *B23* and *C28* mutant lines were isolated from the ethyl methanesulphonate (EMS) mutagenesis screen described in (Barbosa et al., 2007). Homozygous animals from both lines survive until first instar larvae.

Immunohistochemistry and fluorescent in situ hybridization

Embryos were laid at room temperature, dechorionated in 50% bleach for 3 minutes, fixed for 20 minutes in 4% formaldehyde in PBS/heptane, devitellinized using heptane/methanol, and stained using standard protocols. For fluorescent *in situ* hybridization, embryos were fixed in 5% formaldehyde and *in situ* was carried out according to (Lecuyer et al., 2008) using a DIG-labelled RNA probe transcribed from a *412* clone. Primary antibodies were used at the following dilutions: rabbit anti-Vasa (1:10,000) courtesy of Ruth Lehmann, mouse anti-Eya (1:12) from the Developmental Studies Hybridoma Bank (DSHB), mouse anti-FasciclinIII (1:50) from the DSHB, mouse anti-Robo (1:10) from the DSHB, mouse anti-Abd-B (1:10) from the DSHB, rat anti-Vasa (1:40) from the DSHB, mouse BP102 (1:1000) from Abcam (ab12455), sheep anti-digoxigenin:POD (1:250) from Roche, rabbit anti phosphohistone H3 (Ser10) (1:500) from Upstate (Millipore), rabbit anti-Nmr2 (1:1000) from Sandra Leal, rabbit anti-Lola (1:50) from Edward Giniger, guinea pig anti-Traffic jam (1:10,000) from Dorothea Godt, rabbit anti-Srp (1:1000) from Rolf Reuter, and rabbit anti-Tinman (1:1000) from Manfred Frasch. Alexa488 (Invitrogen), Cy3, Cy5 and Biotin (Jackson ImmunoResearch) conjugated secondary

antibodies were used at 1:500. Fluorescent *in situ* signals were detected using the tyramide signal amplification kit (Invitrogen).

Fluorescently stained embryos were mounted in aquamount (Polysciences) and visualized using an Olympus FV1000 confocal microscope with UPlanSApo 20x (NA 0.75) or 60x water (NA 1.2) objectives or a Zeiss LSM710 confocal microscope with 63x objective (NA 1.4). Images were analyzed using ImageJ (NIH) and Imaris 6.1.5 (Bitplane).

Biotinylated secondary antibodies were visualized using a Vectastain ABC Kit (Vector Labs) and 3,3′-Diaminobenzidine, dehydrated and mounted in Epon resin and viewed on a Zeiss AxioImager.

Riboprobes were prepared from wild type cDNA using the primers: for the *lola-B* specific exon: CTGAGTATTACGCGTATAGCGGGACTC and CGAGAAGTGGGGATGCAACTCC, *lola-R* specific exon ATTTGAGCAGGAAGGAGAACACCG and TTATTTGGTTTCAAGCTCTCCCTTCC, *bagpipe*: CGGCCTCTACAAGCTGACCCAACC and TCCGCCGCCGAGTGAACG. The DNA was cloned into the vector pCR™II-TOPO (Invitrogen) and used as a template for RNA probe synthesis using the Digoxigenin RNA labeling kit (Roche) with SP6 RNA polymerase.

The *412* riboprobe was made by amplification of 412 DNA from a pBluescript vector clone (gift from Akira Nakamura) with T3 and T7 primers which was used as a template for RNA probe synthesis with T7 RNA polymerase.

Production of *UAS-lolaR-GFP* and *D-Six4Gal4* flies

The *lola-R* coding sequence was amplified from cDNA using the primers: CACCATGGATGACGATCAGCAGTTTTGTTTG and TTTGGTTTCAAGCTCTCCCTTCCC and cloned into cloned into the pENTR™/D-*TOPO*® vector (Invitrogen), sequence verified and then moved into the destination vector pUASt-*att*B-WG (for production of C-terminal GFP fusions, gift of Saverio Brogna) using the Gateway® reaction. This vector was used to transform flies using phiC31 integrase-mediated site specific recombination using an *attP* site on the third chromosome at position 99F8 (line VK00020).

D-Six4Gal4 was made by amplifying the Gal4VP16 fragment from the nos-Gal4VP16 vector, then cloning it into KpnI/NotI sites in the pD-Six4III Colorless Pelican vector (Sano et al., 2012) and was integrated into the fly genome by P-element-mediated transformation.

Next generation sequencing and alignments

B23 and *C28* mutant lines were isogenized, homozygous embryos collected and genomic DNA isolated. 3µg genomic DNA was sheared into 500bp fragments, paired-end libraries were prepared and subjected to 100bp paired-end Illumina sequencing. The obtained reads were analyzed using the CLC Genomics Workbench software, versions 4.7-5.5. Using the Genomic Gateway plugin tool (now integrated into the software as the 'NGScore tools'), the reads from the three mutants were mapped onto the reference sequence for the 2L and 2R chromosome arms (GenBank NT_033779 and NT_033778 respectively, release 5.30). Coverage for *B23* and *C28* was 19x and 13x for 2L and 2R respectively. Single nucleotide polymorphisms (SNPs) between the mutant reads and the reference genomic sequence were identified and those common between the mutants (and therefore present on the pre-mutagenesis chromosome) were discarded.

Protein sequences were obtained by BLAST searches and alignments were made using ClustalW, and displayed in JalView.

Results

Characterisation of two mutants affecting germ cell migration

In an ethyl methanesulphonate (EMS) mutagenesis screen (described in Barbosa et al., 2007), two zygotic mutants were identified, *B23* and *C28*, exhibiting a defect in germ cell migration, visualized by staining embryos for the germ cell marker Vasa. Although the mutant embryos show wild type early germ cell migration and the germ cells move into the mesoderm normally at stage 11 (Figure 1A-C), by stage 13 the germ cells don't align in a row, but instead appear scattered

(Figure 1D-F). This mismigration is exaggerated at later stages where the germ cells fail to cluster to form a gonad, but are instead scattered at the posterior of the embryo, either as single germ cells or clumped together in several clusters, or forming an uncompacted gonad (Figure 1G-I). These two mutants therefore result in a late misalignment of the germ cells.

B23 is an allele of *midline*

To identify the causative mutations in the two lines, deficiencies that failed to complement the mutants were identified and whole-genome sequencing was used to identify SNPs. *B23* was lethal in trans to deficiency line *Df(2L)Exel6012* and this line was therefore tested for phenotypic complementation. Since B23 and C28 generate a spectrum of gonad defects, like many mutants that affect gonad formation (Weyers et al., 2011), the phenotypes of *B23*/*Df(2L)Exel6012* transheterozygous embryos were scored and compared to *B23* homozygous mutant gonads (Figure 1M). The categorization was performed on stage 15-16 embryos using Vasa-labelled germ cells as a read out of the condition of the gonad. 'wild type' is defined as a pair of round gonads, with 6 or fewer germ cells scattered outside. '≥7 germ cells (gc) outside gonad', included embryos were there are many scattered germ cells, but with a clear gonad on each side. The '≥2 germ cells (gc) clusters' category includes embryos where the germ cells are present as 2 or more neighboring clumps, possibly representing unfused SGP-germ cell clusters. The most severe 'no gonad' category is scored when there are many separate germ cell clusters each containing only a few germ cells and no gonad can be identified. The final category, 'uncompacted gonad', includes embryos where the gonads are visible, but remain elongated at late stages, indicating a failure of gonadal coalescence.

Similar to the *B23* homozygotes, the majority of *B23*/*Df(2L)Exel6012* embryos displayed the most severe category of 'no gonad' (Figure 1M). This implicated the cytological region 25D5-25E6, as defined by the breakpoints of the deficiency, as the causative locus for the *B23* mutant phenotype. This region contained only one SNP from the whole genome sequencing that would be predicted

to cause a coding sequence change. This SNP was in the gene *midline (mid)* and would convert the AG splice site acceptor in the 3rd and final intron to a non-functional AA.

To verify this as the causative mutation two further *mid* mutant alleles were tested for complementation. *mid*[*1*] and *mid*[*2*] have early stop codon mutations and are null alleles (Liu et al., 2009). *mid*[*1*] and *mid*[*2*] were lethal with *B23* and both alleles showed gonad formation defects in trans to *B23* with near identical penetrance and severity, to that in *B23* homozygotes (Figure 1J,M and data not shown). These results demonstrate that *B23* is an allele of *mid,* and hence hereafter will be referred to as *mid*[*B23*].

mid (also called *neuromancer2*) encodes a transcription factor belonging to the Tbx20 (T-box 20) family (Buescher et al., 2004), and has been implicated in various aspects of development including segment polarity (Nusslein-Volhard et al., 1984), heart formation (Miskolczi-McCallum et al., 2005; Qian et al., 2005), neuroblast specification (Buescher et al., 2006) and axonal pathfinding (Liu et al., 2009).

To identify the effects of the *mid*[*B23*] splice acceptor site mutation on the splicing of the *mid* transcript, RT-PCR was performed using RNA from wild type and mutant embryos. On sequencing the transcript from *mid*[*B23*] we observed a 30bp deletion immediately following the 2nd exon. An internal cryptic acceptor site inside the 3rd exon led to restoration of the reading frame, resulting in a 10 amino acid internal deletion within the T-box domain (Figure 1N). To ascertain if the deleted residues were conserved and therefore likely to be important for function, the *D. melanogaster* Mid protein sequence was aligned with closely related T-box proteins from *Drosophila* (*H15*), mosquito (Tbx20), and mouse (Tbx1 and Tbx20). The 10 amino acids predicted to be deleted in the *mid*[*B23*] mutant are very highly conserved thus we would expect the mutant protein to be non-functional (Figure 1P).

C28 **is an allele of** ***longitudinals lacking***

C28 was lethal in trans to the deficiency *Df(2R)BSC595* and therefore this deficiency line was tested for phenotypic complementation. *C28* homozygous embryos displayed 90% mutant gonads covering the whole array of phenotypes (Figure 1M). Nearly 50% of the homozygous embryos showed the most severe class of phenotype, 'no gonad'. Embryos containing *C28* in trans to *Df(2R)BSC595* showed gonadal defects with penetrance of 80%, similar to homozygous *C28* mutant embryos (Figure 1M) indicating that the causative mutation in *C28* lies within the region deleted in *Df(2R)BSC595*. These transheterozygotes displayed a shift of the most represented category to the less severe '≥7 gc outside gonad', indicative of a second site enhancer mutation in the C28 mutant that contributes to the gonad formation defects.

Further deficiency analysis in the region uncovered by *Df(2R)BSC595* mapped the mutant to lie within the smaller deficiency *Df(2R)ED2098*, implicating the cytological region 47A7-47C6, as defined by the breakpoints of this deficiency, as the causative locus for the *C28* mutant phenotype. From the whole genome sequencing data, this region contained only one SNP that would be predicted to cause a coding sequence change, a missense mutation in the gene *longitudinals lacking (lola)*.

To verify this SNP as the cause of the phenotype, a *lola* allele, *lola*[*22.05*], was used to check for complementation. *C28* in trans to *lola*[*22.05*] was lethal and the germ cells of such embryos revealed gonad defects similar to that seen in *C28* homozygotes (Figure 1K,M). Therefore, the *C28* mutation is an allele of *lola*, hereafter referred to as *lola*[*C28*].

lola encodes a transcription factor with more than 30 different predicted protein isoforms, of which at least 20 have been experimentally verified (Giniger et al., 1994; Goeke et al., 2003). All of the isoforms share a common N-terminal domain containing a Broad complex, Tramtrack, Bric-a-Brac (BTB) protein dimerization domain, whereas alternate splicing leads to the varying C-termini (Ohsako et al., 2003). The isoform-specific C-termini typically contain either one or

two zinc-finger motifs of the typical C2H2 or the atypical C2HC class (Goeke et al., 2003).

The mutation in *lola*[*C28*] is predicted to affect only two isoforms, *lola*-G and *lola*-R (Flybase nomenclature), also referred to collectively as *lola4*.7 (Giniger et al., 1994) or *lola*-T (Goeke et al., 2003). The relationship between the various published nomenclature of *lola* isoforms used in this study is given in table 1. *lola*-G and *lola*-R differ in their 5' and 3'UTR, however, they have identical coding sequences and therefore will hereafter be referred to as *lola*-R. Along with the N-terminal BTB dimerization domain, *lola*-R encodes a unique C-terminus with 2 Zn-fingers, one C2HC- and the other C2H2-type (Figure 1O). The mutation in *lola*[*C28*] would cause an asparagine to isoleucine change at position 835, lying within the second Zn-finger motif.

To ascertain if the mutated asparagine residue is conserved and a likely important residue, the *D. melanogaster* Lola-R sequence was aligned with another *D. melanogaster* Lola isoform (Lola-B and Lola-C, with both having identical coding sequences and hereafter termed Lola-B) as well as Lola homologues from other insect species (Figure 1Q). As expected, the two cysteines and histidines forming the finger were highly conserved. The asparagine can be histidine, as in Lola-B and other isoforms (see also Goeke et al., 2003), but is never an isoleucine. Moreover, crystallization studies performed on the DNA-binding domain of Tramtrack protein, one of the first identified members of the BTB domain containing Zn-finger transcription factor, show the importance of the Asn residue for contacting the target DNA (Fairall et al., 1993). Thus the mutation in *lola*[*C28*] gives us an isoform specific *lola* allele, that would likely affect the functionality of the encoded Lola-R protein.

Three alleles of *lola* were recently isolated in a screen performed in search of gonad formation mutants (Weyers et al., 2011). Sequencing one of these alleles, *lola*[*22.05*], revealed a mutation converting the 97th amino acid of the protein from Gln to a stop codon (data not shown). This premature stop early within the common region of Lola leads to loss of all Lola isoforms and therefore this allele is a null (verified by the absence of staining using a pan anti-Lola antibody, recognizing

all isoforms of Lola, data not shown). *lola*[*22.05*] homozygous mutant embryos have a similar penetrance and range of gonad defects as compared to *lola*[*C28*] transheterozygotes (Figure 4K) suggesting that Lola-R is the critical isoform required for gonad formation.

To examine whether other characterised isoforms of *lola* are required for gonad formation we tested whether a specific mutant for isoform *lola*-B, *lola[ORE119]*, also displayed gonad formation defects. Although this allele is lethal in trans to *Df(2R)BSC595* the gonads in such embryos were wild type indicating that this isoform has no essential role in gonad formation (Figure 1L).

Mid and Lola affect SGP behaviour

To investigate if the SGPs were correctly specified, the expression of an early SGP marker (*412* retrotransposon, Brookman et al., 1992) was investigated in *lola* and *mid* mutant embryos. Similar to wild type stage 12 embryos, 3 distinct clusters of SGPs were observed in the mutants, and the migrating germ cells established contact with the SGP clusters (Figure 2B-D, white arrow heads). This showed that the early steps of gonad formation, namely SGP specification and contact formation, were normal in the both the *lola[C28]* and *mid[B23]* mutants.

In subsequent stages in wild type embryos, the three clusters of SGPs fuse into one contiguous tissue (Figure 2A,E). In homozygous mutants, however, the SGP clusters did not always fuse. In most cases, minimally one cluster (typically, but not necessarily, the anterior cluster) was disjoined from the other two clusters. Moreover, many germ cells at stage 13 were scattered in the vicinity of the gonad and were not always associated with the SGPs (Figure 2F,G).

At stage 15, while wild type gonads coalesced into a tight and round gonad (Figure 2A,H), the mutant gonads appeared abnormal. The earlier lack of SGP cluster fusion or ensheathment was not overcome with time (Figure 2I,J), indicating that these processes were defective in the mutants, and not caused simply by a delay in development. Moreover, SGP clusters that were occupied with germ cells did not compact and remained elongated into the later stages of gonad morphogenesis. Therefore *mid* and *lola* homozygous mutants display defects in

many of the SGP-driven processes required for gonad formation. To verify that these defects were not a consequence of secondary mutations on the original chromosomes trans-heterozygous embryos were also scored and defects in SGPs were also observed (Figure 4B, F).

We wanted to test if the lack of ensheathment was due to inability of the mutant SGPs to make protrusions in order to surround the germ cells. We looked at the status of actin using a Moesin-GFP construct (the actin binding domain of Moesin fused to GFP) expressed under the *D-six4* promoter to drive expression in the SGPs (*D-Six4>moeGFP;* Sano et al., 2012*)*. In control stage 13 embryos, actin rich protrusions could be visualized surrounding the germ cells (Figure 2K, inset). We observed a lack of such protrusions in both the *mid* and the *lola* transheterozygous mutant SGPs at this stage (Figure 2L, M, insets), which could further explain the lack of ensheathment observed in these mutants. Quantitative analysis performed on the penetrance of ensheathment of germ cells in five stage 13 embryos of each genotype, where ensheathment was defined when at any given plane of a germ cell a ring of SGP cytoplasm could be seen encircling it, revealed that while in control gonads 100% of the germ cells (n=63) were ensheathed, this was 3% (n=66) and 6% (n=69) in *mid* and *lola* mutants respectively.

To test if the SGP cluster fusion defect in the mutants is due to lack of fusion-competence of mesoderm-derived tissues in general, the integrity of the visceral mesoderm was verified. Similar to the SGPs, visceral mesoderm cells are specified in clusters which fuse during stage 12 to form a single contiguous tissue, that will eventually surround the gut (Azpiazu and Frasch, 1993). In the mutants at stage 13 the visceral mesoderm appeared as a single continuous tissue, which was indistinguishable from wild type (Figure 2K-M, white arrow). This indicates that in the two mutants the mesoderm is fusion competent and the lack of fusion of the mutant SGPs is not due to general mesodermal defects.

lola-R and Mid are expressed in the gonad

To determine the expression pattern of *lola* and *mid* with respect to SGPs and germ cells, antibody stainings and fluorescent *in situ* hybridization were performed on whole mount embryos.

in situ hybridization using a probe to the R-specific exon of *lola* demonstrated that *lola-R* is expressed in both the SGPs and germ cells as well as being abundant in surrounding mesodermal cells (Figure 3A). Another *lola* transcript, *lola-B,* alleles of which displayed no gonad formation defects (Figure 1L), was not detected in SGPs or germ cells (Figure 3B), demonstrating that the gonad expression of *lola-R* is specific.

To detect the Lola protein, an antibody made against the common region of Lola was used, which would label all Lola isoforms (Giniger et al., 1994). The strongest signal was in the CNS, similar to previously published data (Cavarec et al., 1997; Giniger et al., 1994) and that observed by *in situ* hybridization using a probe against the common region (Giniger et al., 1994; and data not shown). In stage 13 embryos, nuclear Lola protein was detected co-localizing with the SGP marker Eya and was detected in germ cell nuclei (Figure 3C). Therefore Lola is expressed in both germ cells and SGPs.

To verify if the Lola-R protein was expressed in the gonad, GFP expression was examined from a bacterial artificial chromosome (BAC) insertion of the *lola* genomic locus with a GFP-tag inserted 3' of the R-specific exon of *lola*. To avoid possible enhanced perdurance of maternally supplied protein, embryos inheriting a paternal copy of the BAC were studied. GFP was observed in the mesoderm of early embryos and in later stage embryos in the SGPs (Figure 3D), brain lobe and salivary glands, which correlates with the *lola-R* RNA expression pattern (data not shown). We did not however detect Lola-R GFP in the germ cells even when the BAC insertion was inherited maternally (data not shown).

mid RNA is expressed in 14 ectodermal stripes, neuroblasts and in the heart (Buescher et al., 2004; Miskolczi-McCallum et al., 2005) but is also visible as 3 clusters in stage 12 embryos in a region where the SGPs would be located

(Miskolczi-McCallum et al., 2005). Mid protein expression has been detected in ectodermal stripes in early embryos, and the heart and the CNS in later embryos but Mid was not reported to be expressed in SGPs (Leal et al., 2009). We labelled wild type embryos using a Mid antibody which showed co-labeling with a nuclear SGP maker, Eya (Figure 3E). We conclude that Mid is expressed in SGPs.

Mid and Lola are required in the mesoderm for proper SGP behaviour

To prove that Mid and Lola are required autonomously in the SGPs, we attempted to rescue the defects of *mid* or *lola* mutant embryos by expressing wild type versions of the respective proteins using a *twiGal4* driver, and in the case of *mid* also a *D-Six4Gal4* driver. The *twiGal4* driver results in early mesodermal expression which is inherited by the SGPs resulting in expression of the transgene in this tissue until stage 15 (as determined using a UAS-GFP control construct, our unpublished results), and has been used to manipulate SGP gene expression (Kitadate and Kobayashi, 2010). The *D-Six4Gal4* driver is more specific to SGPs but results in relatively late expression as compared to *twiGal4* (our unpublished results).

The *mid*[*1*] *twiGal4* chromosome when heterozygous did not show gonad defects (Figure 4A, D). *mid*[*1*] *twiGal4*/*mid*[*B23*] trans-heterozygous embryos on the other hand displayed severe gonad formation defects, similar to that in *mid*[*B23*] homozygotes (Figure 4B, D). On mesodermal expression of *mid*, in such a *mid* mutant background (*mid*[*1*] *twiGal4*/*mid*[*B23*]; *UASmid* embryos), the SGP-related defects, including the lack of fusion of the SGP clusters and the ensheathment of the germ cells by the SGPs, were fully rescued and the numbers of scattered germ cells at this stage were also reduced (Figure 4C, D). On using the *D-Six4Gal4* driver (*mid*[*1*] *D-Six4Gal4*/*mid*[*B23*]; *UASmid* embryos), the SGP-related defects in the majority of embryos were rescued, but not to the extent as seen with *twiGal4,* most likely due to the later onset of *mid* expression using this driver. These data demonstrate that Mid is required in the SGPs for normal gonad morphogenesis.

For the rescue of *lola*, scoring of the phenotypes was aided by the presence of the *68-77* SGP *lacZ* enhancer trap on the *lola*[*22.05*] *twiGal4* chromosome. Due to this the last two categories of '≥2 germ cells (gc) clusters' and 'no gonad' was replaced by '≥2 SGP clusters/gonad'. In embryos heterozygous for the *lola*[*22.05*] *68-77 twiGal4* chromosome the gonads were wild type whilst *lola*[*22.05*] *68-77 twiGal4/lola*[*C28*] trans-heterozygous embryos showed a high penetrance of gonad defects similar to that observed in *lola*[*C28*] homozygotes (Figure 4E, F,K).

Expressing *lola-R-GFP* was able to rescue the gonad defects of *lola*[*22.05*] *68-77 twiGal4/lola*[*C28*] trans-heterozygotes, leading to round and compact stage 15 gonads and few lost germ cells (Figure 4G,K). This proves that Lola is required in the mesoderm and not the germ cells. To support this conclusion we made germ-line clones using the *lola*[*C28*] allele to remove the maternal (and hence germ cell) contribution. Such embryos displayed wild-type gonads indicating that maternal *lola-R* is not essential for gonad formation (Figure S1). In support of this conclusion we also mis-expressed Lola-R-GFP in the germ cells (using the *nosGal4VP16* driver) and this did not disrupt germ cell migration or gonad formation (Figure S1).

The Lola-R isoform is sufficient for gonad function

We also attempted to rescue the gonad defects of *lola* trans-heterozygotes with another *lola* isoform, *lola-B,* also encoding a functional Lola isoform containing a BTB dimerization domain and two Zn-finger DNA-binding domains (Goeke et al., 2003). Mesodermal *lola-B* expression was, however, unable to rescue the phenotype (Figure 4H,K). This inability was not due to dominant effects of over-expression, as has been reported for dendrite targeting of projection neurons (Spletter et al., 2007), because mesodermal expression in a wild-type background did not affect gonad formation (Figure 4I,K).

To test whether the R isoform is sufficient to supply all Lola function to SGPs we expressed the *lola*-R isoform in the mesoderm of *lola* null mutants (homozygous *lola[22.05]* embryos) (Figure 4J,K). Such expression was able to rescue all gonadal defects. Taken together these data demonstrate firstly that the *lola*-R isoform is

both necessary and sufficient to supply Lola function to SGPs. Secondly, the functions performed by the Lola-R isoform cannot be replaced by another Zn-finger containing isoform and suggests that Lola-R has specific downstream targets which cannot regulated by another Lola isoform.

mid but not *lola*[*C28*] mutants show defects in axonal tracts in the VNC

Midline mutant embryos display defects in the ventral nerve cord (VNC) (Liu et al., 2009). Null mutants of *lola*, containing lesions in the common exons also reportedly show defects in the VNC, with a loss of longitudinal axons (Crowner et al., 2002; Giniger et al., 1994; Madden et al., 1999). The disruptions in the longitudinal tracts of the VNC in *lola*[*22.05*] (Figure S2C), confirmed the phenotype seen previously in other *lola* null mutants. To ascertain if the *lola* isoform required for SGP behaviour is also required in the VNC, the axonal scaffolds of the VNC of *lola*[*C28*] mutant embryos were examined. Interestingly, when compared to the null *lola[22.05]* allele, *lola*[*C28*] mutants had wild type axonal tracts (Figure S2D).

This data indicates not only that *lola-R* is not required for VNC development but also demonstrates that we have uncovered an isoform specific allele of *lola* which uncouples its function in nervous system development and gonad development.

mid[*B23*] mutants also displayed severe interruptions in the longitudinal axonal tracts (Figure S2B), which appeared similar in strength to the published null alleles of *mid* (Liu et al., 2009), affirming that the *mid*[*B23*] allele is a null.

Mid is required for robust Traffic Jam expression

Tj is a MAF family transcription factor expressed in both the VNC and SGPs and is required for germ cell ensheathment (Li et al., 2003). As one of the defects in *mid*[*B23*] mutants is the lack of germ cell ensheathment, in spite of early SGP-germ cell contacts, we tested whether Tj expression was affected by loss of Mid.

In *mid* heterozygous control embryos, robust Tj expression was observed in the nucleus of all SGPs from stage 13 onwards (Figure 5A), with an average of 34 Tj expressing SGPs per gonad (n=5 gonads). In contrast, in stage 13 *mid*[*1*] *twiGal4*/*mid*[*B23*] trans-heterozygotes very few or no SGPs expressed Tj (Figure 5C), with an average of 1 Tj expressing SGP per gonad (n=10 gonads). At stage 15, the number of Tj expressing SGPs was greater than at stage 13, with an average of 8 Tj expressing SGPs per gonad (n=10 gonads) (Figure 5D) but still much less than control gonads which had an average of 35 Tj-expressing SGPs per gonad (n=5 gonads).

The effect of *mid* on Tj expression was specific to SGPs because expression of Tj in the VNC was unaffected in *mid* mutants (Figure 5A, C insets). The loss of Tj expression is not a secondary consequence of lack of SGP fusion and coalescence because *lola*[*C28*] mutants displayed wild type SGP Tj expression (Figure 5G, H).

To test if Mid is required autonomously in SGPs for robust Tj expression, we examined Tj expression in *mid* mutant embryos rescued with mesodermally driven Mid. The gonads in the *mid*[*1*] *twiGal4*/*mid*[*B23*]; *UASmid* rescue embryos showed robust Tj expression from stage 13 (Figure 5E, F) indicating that mesodermal expression of Mid is sufficient to rescue Tj expression in the SGPs.

To determine whether the few Tj positive SGPs in late stage *mid* mutants were anterior or posterior SGPs we counterstained *mid*[B23] mutant gonads with an anti-AbdB antibody. Abd-B is expressed by a small subset of SGPs localized to the posterior of the gonad. We found that the SGPs expressing Tj can be AbdB positive (27%) or negative (73%) (Figure S3, overall 22 TJ positive SGPs in 6 embryos), therefore there is no bias for anterior versus posterior SGPs for those that express Tj.

Tinman unidirectionally regulates Mid expression in SGPs

Tin is an early expressed transcription factor required for the proper differentiation of several mesodermal tissues (Azpiazu and Frasch, 1993; Bodmer, 1993). In the heart Tin is required to directly activate *mid* expression (Miskolczi-

McCallum et al., 2005; Ryu et al., 2011) and conversely, Mid is later required to maintain Tin expression in 4 out of the 6 cardioblasts per hemisegment (Reim et al., 2005), see also Figure 6C, F). Tin is also required for SGP specification and maintenance (Boyle et al., 1997). Although *tin* is expressed in all mesoderm until stage 9, from stage 10 it is restricted to the dorsal mesoderm, and is not reported to be expressed in the SGPs (Azpiazu and Frasch, 1993; Bodmer, 1993; Yin et al., 1997).

To test if Tin is expressed by SGPs and is downstream of Mid, wild type gonads were analyzed for Tin expression using an anti-Tin antibody. Surprisingly, Tin expression was detected in all SGPs in stage 13 embryos but by stage 15 its expression was highest in the anterior most SGPs (Figure 6A, B). In stage 13 *mid*[*B23*] mutants expression of Tin was observed similar to wild type (Figure 6D). Similarly, in mutant stage 15 gonads, Tin expression could be observed in cells making contact with the germ cells, however, no differences in Tin levels could be seen in the stage 15 SGPs, indicating that differences in Tin expression levels between SGPs in wild type may require correct gonad assembly (Figure 6E).

Although Mid was not required for Tin expression in the SGPs, we tested whether Tin was required for Mid SGP expression, similar to what is observed in the heart (Azpiazu and Frasch, 1993; Bodmer, 1993; Van Doren et al., 1998). While *tin* is necessary for SGP specification, in *tin* mutants, a few SGPs are specified and maintain SGP identity (Boyle et al., 1997; Broihier et al., 1998). In *tin[346]* mutant gonads, we did not detect Mid expression in the few surviving SGPs as judged both by anti-Mid antibody staining (Figure 6G, observed in 4 of 4 gonads) and by use of a *mid>lacZ* reporter (Figure S4). These *tin[346]* mutant SGPs also lacked Tj expression (Figure 6H, 9 gonads had no Tj positive SGPs, 2 gonads had just one or two Tj positive SGPs of the more than 15 SGPs in each), as would be expected from our previous result that Mid is required for Tj expression in SGPs.

We conclude that a linear hierarchical relationship exists between Tin, Mid and Tj in the SGPs, which is different to that observed in the heart.

Robo is not downstream of Lola or Mid

The receptor Robo is implicated in gonad formation at the step of SGP cluster fusion and gonadal compaction (Weyers et al., 2011). Moreover, both Mid (Liu et al., 2009) and Lola (Crowner et al., 2002) regulate Robo levels in the CNS, making it a likely target in the gonads. In wild type stage 15 embryos, Robo localizes to the cell surface of both SGPs (yellow arrow head) and germ cells (arrow head) (Figure S5). In *mid*[*B23*] and *lola*[*C28*] mutants the Robo signal was seen at the surface of the germ cells (Figure S5). Furthermore, the SGPs of mutants also expressed Robo at levels not distinguishable from wild type gonads. Thus Robo is not downstream of Mid or Lola in the SGPs.

Lola and Mid interact to form super-elongated gonads

Since mutants in *mid* and *lola* display a similar spectrum of gonad defects, we tested whether Mid and Lola fit into a simple linear cascade. We found that Mid is expressed normally in Lola mutants and vice-versa (Figure 7) suggesting these genes act in parallel. In agreement, expression of *lola-R* was not able to rescue *mid*[*B23*] mutant gonads (data not shown). However, on performing the reciprocal experiment, a neomorphic phenotype was produced: Mid over-expression in *lola* mutants led to the formation of 'super-elongated' gonads in more than 50% of stage 15 over-expression embryos (n=48). Although SGP cluster fusion occurs, these gonads remain elongated, spanning several parasegments. (Figure 8A). Staining of the SGPs using the marker Tj revealed far more SGPs as compared to sibling controls (Figure 8B, n=5 gonads) and the expression of another SGP marker, the *412* retrotransposon, was also expanded (Figure 8C-D, n=6 gonads).

We tested whether additional proliferation of the SGPs contributed to their increased number in Mid over-expressing *lola* mutant embryos. Such embryos were stained against phosphorylated-Histone 3 (pH3), a proliferation marker. We found no differences in pH3 labeling of SGPs in stage 12 or 13 embryos between the overexpression and the sibling control, where each genotype scored an average of 12.1% and 11.2% pH3 positive SGPs at these stages respectively (10 gonads

examined for both mutant and sibling control embryos, with total number of SGPs analyzed 363 and 232 respectively) (Figure S6).

'super-elongated' gonads are also formed upon overexpression of the homeodomin proteins Abd-A (Boyle and DiNardo, 1995; Greig and Akam, 1995) or Zfh-1 (Broihier et al., 1998). In the former case, the extra SGPs arise from transformation of fat body cells in anterior parasegements (Riechmann et al., 1998), whilst in the later the additional SGPs occur at the expense of visceral mesodermal cells in parasegements 10-12 (Broihier et al., 1998).

To determine whether the additional SGPs in Mid over-expressing *lola* mutant embryos are originating via one of these two mechanisms, we stained such embryos for Serpent (Srp) and *bagpipe (bap)*, markers for the fat body and visceral mesoderm respectively. We observed no differences in the domain size of *bap* RNA expression between stage 10 over-expression and sibling embryos (Figure 8E-F). Examining Srp in stage 13 overexpression embryos, however, revealed co-expression of the SGP marker Eya and the fat body marker, Srp. This co-expression was observed in only the anterior SGP clusters (Figure 8H, H'), whereas in the posterior, although SGP and fat bodies existed in close vicinity, no overlap in expression occurred (Figure 8H, H''). The anterior SGP clusters in the sibling control embryos, on the other hand, never expressed Srp (Figure 8G, G'). This data indicates that the extra SGPs observed in the late stage 'super elongated' gonads arise from the conversion of some fat body cells into SGPs at stage 13. The fat body cells closest to the SGPs, take on SGP fate and join the existing gonad, giving it the 'super elongated' appearance.

Discussion

Embryonic gonad formation involves a complex interplay between two cell types and is a good model system for studying changes in cellular behaviors and cell-cell interactions, required for organogenesis. In this work we have identified a role for two transcription factors, Lola and Mid, in gonad development.

The *lola* locus encodes for up to 25 differentially spliced annotated isoforms. A previous study had also identified a role for Lola in gonad formation (Weyers et al., 2011), and this work extends this finding in several respects. Firstly we identify *lola*-R as a specific isoform that is required by the gonad during its development. Secondly we show that Lola-R is expressed by the SGPs and mesodermal expression of this isoform can rescue the gonad formation defects of *lola* null embryos. This indicates that Lola-R is required mesodermally, and that this *lola* isoform is sufficient to provide all Lola function in the gonad. Another zinc finger containing Lola isoform was unable to rescue the gonad defects of *lola* mutant embryos indicating functional differences in the distinct Lola isoforms. Whether Lola is required in the SGPs or the surrounding mesodermal cells remains an open question. It remains possible that Lola has cell autonomous functions in the SGPs as well as non-cell autonomous functions in the mesoderm (such as repressing *mid* or Mid function, see below).

Although germ cell *lola*-R is not required for germ cell migration or gonad formation during embryogenesis and the Lola-R protein cannot be detected in these cells, other Lola isoforms are expressed and required in adult germ cells. In testes, *lola*-B and *lola*-I are required cell autonomously for germline stem cell maintenance and differentiation (Davies et al., 2013). In ovaries Lola-I is required for programmed cell death of late stage nurse cells (Paige Bass et al., 2007). However, this requirement for Lola during oogenesis blocks the production of eggs from germ line clones of *lola* null alleles, which prevents us from testing whether other Lola isoforms play a role in embryonic germ cells.

In addition to being required for gonad formation, *lola* is required in the CNS. Mutants for *lola* null alleles show disrupted axonal tracts, however mutants in *lola*-R have wild-type axonal tracts. This reiterates the isoform-specific function of *lola* and demonstrates the ability to genetically uncouple the role of Lola in nervous system and gonad development. The lethality of flies containing the *lola*-R specific mutation in trans to a *lola* null indicates that Lola-R is also required in tissues other than the gonad, as defects in the latter would not be expected to lead to lethality.

The second transcription factor identified in this study was *mid*. Mid is a T box containing transcription factor of the *tbx20* subclass with roles in embryonic patterning and axonal pathfinding (Liu et al., 2009; Nusslein-Volhard et al., 1984). We show that *mid* mutants also have defects in gonad formation and that *mid* is required tissue autonomously by the SGPs.

To search for targets downstream of Mid and Lola in the gonad we tested the expression of genes either already identified as being important for SGP behaviour or known downstream targets in other tissues. Mid and Lola are both reported to be upstream of the cell surface receptor Robo, in the CNS. A Mid consensus binding site in the promoter region of Robo was identified with demonstrated Mid binding by chromatin immunoprecipitation (Liu et al., 2009). However, in the gonad of both *mid* and *lola* mutants Robo expression appeared normal. Furthermore we found no observable differences in Robo levels in the CNS of *mid*[*B23*] or *mid*[*1*] mutants compared to their heterozygous siblings in the same embryo collection. Moreover, a recently published study questioned the binding site proposed by Liu et al. and identified a Mid consensus motif closer to the that of its vertebrate homologue, Tbx20 (Najand et al., 2012). Thus, although Robo is clearly required for gonad formation, whether it is downstream of Mid remains a matter of controversy.

In this study, besides having demonstrated the role of two genes in gonad formation, we have further built upon the transcriptional regulatory map in this tissue. We identified the early SGP expression of Tj as being Mid-dependent. Although we could detect Tin in late SGPs this expression was not dependent on Mid. However, the loss of Mid and Tj expression in *tin* mutant SGPs, revealed a cascade of transcription factors functioning in a hierarchical and stage dependent fashion. Although, a reciprocal relationship exists between Mid and Tin in the heart (Miskolczi-McCallum et al., 2005; Reim et al., 2005), our data demonstrates how tissues derived from the same germ layer can have different regulatory networks between the same genes.

Since Lola and Mid are both transcription factors, they could potentially regulate a common pool of downstream targets. Mesodermal expression of Lola-R-GFP in a *mid* mutant background did not rescue the *mid* mutant phenotype (data not

shown). This indicates that *lola* is not the sole downstream target of *mid* in the gonad. However, Mid over-expression in a *lola* mutant background results in a 'super-elongated' gonad consisting of supernumerary SGPs that span several parasegments even at late embryonic stages. This 'super-elongated' gonad results from additional SGPs being specified at the expense of fat body cells, and mirrors the effect of overexpression of the homeobox containing transcription factor Abd-A (Boyle and DiNardo, 1995; Greig and Akam, 1995). This data raises the possibility that Abd-A balances the relative expression of Mid and Lola and suggests that the number of direct Abd-A targets is rather limited as its over-expression phenotype can be recapitulated by affecting their expression.

Given that Mid and Lola do not contain homeoboxes and are not required for SGP specification or maintenance, the 'super-elongated' phenotype seen upon over-expression of Mid in a *lola* background is surprising. These data argue that Lola functions to oppose Mid. Thus in the presence of wild-type Lola, overexpression of Mid does not affect SGP specification, however, in the absence of Lola, Mid overexpression results in additional SGPs.

A similar situation, of cell fate changes requiring shifts in expression of multiple transcription factors, occurs in the *Drosophila* heart. Heart cell specification requires Nkx (*tin*), GATA (*pannier*) and T box (*mid*, or *Dorsocross*) transcription factors. Whilst mis-expression of each factor alone is not sufficient to induce extra cardiac cells, combinations of these transcription factors (for example over-expression of *Doc2* and *pnr*) can induce numbers of extra cardiac cells (Reim and Frasch, 2005).

Our results suggest that although the transcription factors required by SGPs can ostensibly be assigned to those being required for either SGP specification (such as Tin, Abd-A, Abd-B and Zfh-1) or behaviour (including D-Six4, Tj, Mid and Lola), such transcription factors can also interact to impinge on both processes. Investigating the downstream targets of Mid and Lola will provide new players and clues into how SGPs are specified and then programmed to interact with germ cells and each other to form a functional gonad.

Figure 1: Identification of mutants with gonad formation defects as alleles of *mid* and *lola*.

(A-I) Lateral (A-L) views of stage 11 (A-C), stage 13 (D-F) and stage 15 (G-L) wild type (A, D, G), *B23* mutant (B, E, H), *C28* mutant (C, F, I), B23 transheterozygous (J), C28 transheterozygous (K) and *lola[ORE119]* mutant (L) embryos stained for Vasa to label the germ cells. Insets show one gonad at higher magnification.

(M) Quantification of germ cell phenotypes of the *B23* allele in trans to a *midline* deficiency and null allele (upper panel) and *C28* allele in trans to a *lola* deficiency (lower panel). Categories in are described in the text. *n* indicates number of gonads scored.

(N) Domain structure of the Mid protein showing a N-terminal engrailed homology (EH1) domain and central T-box (Formaz-Preston et al., 2012). The region deleted in the *B23* allele is indicated.

(O) Domain structure of the Lola-R isoform showing the N-terminal region containing a BTB dimerization domain that is encoded by the exon common to all isoforms, and the C-terminal region containing 2 zinc finger domains encoded by an isoform R specific exon. The missense mutation in *lola[C28]* is in the second zinc finger (indicated).

(P) ClustalW alignment of the *Drosophila* Mid (accession NP_608927) region surrounding that deleted in *mid*[*B23*] with Tbx proteins from *Drosophila* (H15, CAA67304), mosquito (Tbx20, XP_001659147) and mouse (Tbx1, XP_358777 and Tbx20, NP_919239). Amino acids showing 100%, 80% and 60% identity are highlighted in dark, medium and light purple respectively. *mid[B23]* results in a 30 nucleotide deletion at the site of the exon 3 - exon 4 boundary which would result in a 10 amino acid deletion (boxed residues).

(Q) ClustalW alignment of the second zinc finger domain of Lola-R (accession NP_524766.2) with Lola-C (NP_724946) and homologs from other insect species including *Drosophila erecta* (XP_001976204.1), *Drosophila virilis* (EDW61745.1), *Aedes gambiae* (XP_001688538.1), *Tribolium castaneum* (NP_001157315.1). Amino

acids showing 100%, 80% and 60% identity are highlighted in dark, medium and light purple respectively. The two cysteines and histidines (asterisks) that co-ordinate zinc, along with the asparagine mutated in *lola[C28]* (arrow) are indicated.

Figure 2: Mid and Lola are required for correct SGP behaviour.

(A) Schematic of gonad formation in wild type embryos. The germ cells are loosely associated with the SGP clusters at stage 12. By stage 13 the SGP clusters fuse and ensheath the germ cells. By stage 15 the gonad compacts and rounds up.

(B-J) Wild type (B, E, H) and *B23* (C, F, I) or *C28* (D, G, J) mutant embryos with SGPs labelled using the *412* probe (red), germ cells labelled using a Vasa antibody (green), and the nuclei using DAPI (blue, B-D). At stage 12 the mutants show 3 clusters of SGPs (white arrow heads), similar to wild type (B-D). At stage 13, the SGPs in mutant embryos fail to align and fuse but germ cells remain in close proximity (E-G). At stage 15 a compact round gonad is not formed in the mutants (H-J). Scale bar = 50μm (D) or 10μm (G).

(K-M) *D-Six4moeGFP/+* control (K, inset) and *mid*[*B23*]/*mid*[*1*] *; D-Six4moeGFP/+* (L, inset) or *lola*[*C28*]/*lola*[*22.05*] *; D-Six4moeGFP/+* (M, inset) embryos with SGPs labelled using a GFP antibody to detect the MoeGFP expressed by the *D-six4* promoter (red), and the germ cells (green) using an anti-Vasa antibody. At stage 13, mutants display a lack of germ cell ensheathment by the SGPs, which, unlike in control embryos, fail to form protrusions. The inset in panel M demonstrates that although three SGPs, numbered 1, 2 and 3, whose cell bodies are labeled using the *D-Six4moeGFP* marker surround a germ cell, however, all three fail to form any cytoplasmic protrusions, made clear by the absence of *D-Six4moeGFP* label encircling the germ cell.

(N-P) Wild type (K) and *mid*[*B23*] (L) or *lola*[*C28*] (M) mutant embryos labelled using a FasIII antibody (red) and nuclei using DAPI (blue), demonstrating a contiguous visceral mesoderm (white arrows). Scale bar = 50μm.

Figure 3: Lola and Mid are expressed by SGPs.

(A-E) Stage 13-15 embryonic gonads with germ cells labelled with anti-Vasa antibody (blue) and SGPs with anti-Tj (A-B) or anti-Eya (C-E) antibodies (red). Arrowheads show expression in SGPs, arrows show expression in germ cells. (A-B) Fluorescent *in situ* hybridization using *lola*-R (A) and *lola*-B (B) isoform specific probes (green). (C) Lola protein (green), detected using an antibody against the N-terminal region common to all isoforms, is expressed in both germ cell and SGP nuclei. (D) SGP expression of GFP (green) from a paternally inherited transgene containing the *lola* genomic locus with GFP inserted into the *lola-R* specific exon. (E) SGP expression of Mid using an anti-Mid antibody. Scale bar = 10μm.

Figure 4: Rescue of *lola* and *mid* gonad defects with mesodermal expression.

(A-C, E-J) Gonads of stage 15 embryos with germ cells labelled with an anti-Vasa antibody (green) and SGPs with either *in situ* hybridisation with *412* probe (A-C, red) or anti-lacZ antibody (E-J, red), due the presence of a SGP specific *lacZ* containing enhancer trap, *68-77,* on the *twiGal4* containing chromosome. In control embryos the gonads have compacted (A, E). In *mid* transheterozygous embryos the SGPs fail to coalesce (B), which is rescued upon mesodermal specific expression of *mid* (C). In *lola* embryos transheterozygous for the *lola-R* specific allele in trans to a null allele, the SGPs fail to fuse (F) which is rescued by expression of the *lola-R-GFP* (G) but not *lola-B* (H) in the mesoderm. Mesodermal expression of *lola-B* does not cause defects in gonad formation in a wild-type background (I). Mesodermal expression of *lola-R* is also sufficient to rescue the gonad defects in homozygous *lola* null embryos (J). Scale Bar = 10μm. (D, K) Graphs quantify the degree of rescue according to the categories described in the text. *n* indicates number of gonads scored.

Figure 5: Mid is required for robust Traffic jam expression in SGPs.

Gonads of stage 13 (A, C, E, G) and 15 (B, D, F, H) embryos with germ cells labelled with an anti-Vasa antibody (blue), SGPs by *in situ* hybridisation with *412* probe (red) and Tj expression (green, grey). Control gonads display robust Tj levels in the SGPs and VNC (arrow in low magnification inset in A') at stage 13 (A) which is

maintained at later stages (B). *mid* transheterozygous embryos show a complete loss of gonad Tj expression at stage 13 (C), in spite of normal expression in the VNC (arrow in low magnification inset in C'). Older embryos display occasional Tj expression in a subset of SGPs (D). The reduction of Tj in the gonad is rescued on mesodermal expression *mid* (E, F). *lola*[*C28*] mutants show normal gonad levels of Tj (G, H). Scale bar = 10μm.

Figure 6: Tinman unidirectionally regulates Mid expression in SGPs.

Wild type (A, B) and *mid* mutant (D, E) gonads showing Vasa-labelled germ cells (blue), SGPs labelled with anti-Tj antibody (red) and Tin expression (red, grey). At stage 13 all SGPs are positive for Tin (C) whereas by stage 15 Tin expression is highest in the anterior SGPs (B). In *mid* mutant embryos, Tin expression is robust, in spite of absent or reduced Tj expression (D, E) (observed in 5 of 5 gonads for both stages).

(C, F) Dorsal views of stage 15 embryos showing Tin expression in 4 out of the 6 cardioblasts per parasegment in wild type (C), but a reduction in the number of cardioblasts expressing Tin in *mid* mutant hearts (F). Scale bar = 10μm.

(G, H) *tin[346]* homozygous mutant stage 13 gonads showing Vasa-labelled germ cells (blue) and SGPs labelled with anti-Eya antibody (red). The few specified mutant SGPs lack Mid (green) (G, G') and Tj expression (H, H') while the sibling control embryos express these transcription factors (insets in G, G', H, H').

Figure 7: Midline and Lola act in parallel.

(A, B) Lola protein (green, gray) is expressed in stage 15 *mid*[*B23*] mutant SGPs labelled using an anti-Tj antibody (red) (A, A'), similar to sibling control embryos (B, B').

(C-F) Mid protein (green, gray) is expressed in stage 13 (C, E) and stage 15 (D, F) *lola*[*C28*] mutant SGPs (C, D) (observed in 4 of 4, and 1 of 1 gonads respectively), labelled using an anti-Eya antibody (red) similar to sibling control embryos (E, F). Vasa-labelled germ cells are in blue.

Figure 8: Increased SGP specification in Mid overexpressing *lola* mutant embryos.

(A-B) Stage 15 gonads stained for germ cells using an anti-Vasa antibody (green) and SGPs using an anti-Tj antibody (red). (A, A') A control embryo over-expressing Mid in the mesoderm in a wild type background does not affect gonad morphology and SGP numbers (compare also to Figure 7B). (B, B') Such overexpression in *lola* transheterozygotes leads to abnormal 'super-elongated' gonads, spanning more that one parasegment, and displaying a greater number of SGPs.

(C, D) Lateral views of late stage 12 embryos labelled using the *412* probe to mark SGPs (green), anti-Vasa antibody to mark the germ cells (red) and DAPI-stained nuclei (blue). The *412* RNA expression is maintained in the overexpression embryos in additional patches (arrowheads) anterior to those seen in wild type at this stage. (100% penetrance on comparing 6 embryos of each genotype). Inset in D shows a dorsal view of a stage 13 embryo emphasizing the expanded *412* expression (arrowheads).

(E, F) Ventral view of LacZ positive (brown) sibling control (n=10) (E) and Mid overexpressing *lola* transheterozygous (100% penetrance on comparing 10 embryos of each genotype). (F) stage 10 embryo showing that the domains of *bap* expression (blue) are not diminished in the mutants.

(G, H) Lateral view of a sibling control (G,G',G'') and Mid overepxressing *lola* transheterozygous (H, H',H'') stage 13 embryo with fat body cells labelled using anti-Srp antibody (geen), SGPs with anti-Eya antibody (red) and germ cells with anti-Vasa antibody (blue). Magnified view of anterior and posterior gonad regions (dashed boxes) are given in G', H' and G'',H'' respectively. Co-expression of Srp and Eya is never observed in control SGP nuclei (observed in 5 of 5 gonads) (arrowhead in G'), however, in the mutant embryos some anterior SGPs express both markers (observed in 9 of 9 gonads) (arrowhead in H'). Scale bar = 10μm.

Supplemental Figure 1: Lola-R is not required in germ cells.

(A-E) Ventral view of stage 15-16 embryos stained for Vasa to label the germ cells. (A-D) Embryos laid by *nosGal4VP16* females (which drives expression in germ cells)

mated to (A) *UAS lacZ* (control), (B) *UAS lola-R-GFP*, (C) *UAS lola-L* and (D) *UAS mid* males show no defects in gonad formation. (E) Embryo laid by *lola[C28]* germ line clones females which therefore lack functional maternal (denoted M-) (and hence germ cell) *lola-R* showing wild type gonads.

Supplemental Figure 2: The *lola-R* isoform is not required for axonal pathfinding in the embryonic VNC.

(A-D) Ventral view of stage 16 embryos showing the axonal scaffold of the VNC stained using the antibody BP102 (green). While the longitudinal tracts (white arrow head) in the VNC of wild type (A) embryos are intact, in the null mutants *mid[B23]* (B) and *lola*[*22.05*] (C) severe disruptions in these tracts are observed. However, in the *lola-R* specific mutant, *lola[C28]*, the axonal tracts appear wild-type (D). (observed with 100% penetrance in 5 embryos of each genotype mentioned). Scale bar = 10μm.

Supplemental Figure 3: Tj expressing SGPs in late *mid* mutant gonads can be both anterior and posterior SGPs.

Sibling control (A) and *mid[B23] / Df(2R)Exel6012* (B) stage 15 gonads stained for Vasa (blue), Abd-B (green) and Tj (red). In wild type, a subset of SGPs located towards the posterior or the gonad are positive for Abd-B. In *mid* mutants, the few SGPs that express Tj can be both Abd-B positive (arrow heads) and negative (arrow). Sibling embryos were identified by lacZ expression from a *ftz>lacZ* transgene also in the blue channel resulting in weak staining of some somatic cells. Gonad is outlined by dashed lines. Scale bar = 10μm.

Supplemental Figure 4: Mid is not expressed in *tin* mutant SGPs as judged using a Mid reporter construct

Stage 15 sibling control (A) and stage 14 *mid>lacZ ; tin[346]* (B) gonads stained for Vasa (blue), lacZ (red) and Eya (green). Note that the secondary antibody used to detect the antibody against Eya has species cross-reactivity to the antibody against Vasa causing germ cells to also be highlighted in this channel. In the sibling control

LacZ staining is visible in the SGPs (arrows) whereas in the *tin* mutant embryos the few remaining SGPs (arrow) are LacZ negative. Scale bar = 10μm.

Supplemental Figure 5: Robo levels are unaffected in *mid*[*B23*] and *lola*[*C28*] mutants.

In wild type stage 15 (A, A') Robo (red, gray) expression is observed in both Vasa-labelled germ cells (green) (A' arrows) and closely associated cells, SGPs (A' arrow head). Similar to wild type, *mid*[*B23*] (B, B') and *lola*[*C28*] (C, C') mutant gonads also display germ cell (B', C' arrows) and SGP (B', C' arrow head) specific Robo expression (observed in 4 of 4 gonads for each mutant). Scale bar = 10μm

Ventral view of stage 16 sibling control (D, F), *mid[B23]* (n=4 embryos) (E) and *mid[1]* (n=6 embryos) (G) homozygous mutant embryo showing Robo staining in the VNC. Although axonal tracts are disrupted in the mutants (yellow arrowheads), there is robust Robo staining.

Supplemental Figure 6: Increased SGP number in Mid overexpressing *lola* mutant embryos is not due to increased SGP cell proliferation.

(A-D) Maximum projection of several confocal sections of a lateral view of stage 12 (A-B) and 13 (C-D) embryos stained using an anti-phosphohistone H3 (pH3) antibody to mark mitotic cells (green), and an anti-Eya antibody to mark the SGPs (red). Arrows indicate all co-localizing pH3 and Eya signals based on analysis of single sections. Other apparently overlapping signals are actually in different focal planes. SGPs in mitosis are observed at similar rates in stage 12 sibling control (A,C) and Mid over-expressing *lola* transheterozygous embryos (B,D).

This paper	Flybase transcripts	Other published names	Isoform specific allele
lola-R	*lola-RR, lola-RG*	*lola 4.7* (Giniger et al. 1994) *lola-T* (Spleter et al. 2007)	*lola[C28]*
lola-B	*lola-RB, lola-RC*	*lola-L* (Spleter et al. 2007)	*lola[ORE119]*

Table 1: Lola isoform nomenclature for isoforms used in this study

Acknowledgements

We thank members of the lab including Jennifer Bergmann, Amrita Mukherjee, Tina Bresser, Kristina Ile and Matthias Schneider for comments on the manuscript. We would also like to thank Uwe Irion for helpful discussion. The *lola[C28]* and *mid[B23]* alleles were obtained in a screen for germ cell migration mutants performed in the lab of Ruth Lehmann coordinated by Vitor Barbosa. We acknowledge the DSHB, maintained by The University of Iowa, Department of Biology, as a source of several of the antibodies used in this work. We also acknowledge the Flybase consortium and Bloomington stock centre at Indiana University for gene and stock curation and fly stocks respectively. We thank the labs of Mark Van Doren, Rolf Reuter, Edward Giniger, Sandra Leal, Dorothea Godt, Manfred Frasch and William Brook for reagents. The authors declare no conflicts of interest.

Abbreviations List

SGP, somatic gonadal precursor cell
VNC, ventral nerve cord
CNS, central nervous system

Azpiazu, N., Frasch, M., 1993. tinman and bagpipe: two homeo box genes that determine cell fates in the dorsal mesoderm of Drosophila. Genes & Development 7, 1325-1340.

Barbosa, V., Kimm, N., Lehmann, R., 2007. A maternal screen for genes regulating Drosophila oocyte polarity uncovers new steps in meiotic progression. Genetics 176, 1967-1977.

Bodmer, R., 1993. The Gene Tinman Is Required for Specification of the Heart and Visceral Muscles in Drosophila. Development 118, 719-729.

Boyle, M., Bonini, N., DiNardo, S., 1997. Expression and function of clift in the development of somatic gonadal precursors within the Drosophila mesoderm. Development (Cambridge, England) 124, 971-982.

Boyle, M., DiNardo, S., 1995. Specification, migration and assembly of the somatic cells of the Drosophila gonad. Development 121, 1815-1825.

Broihier, H., Moore, L., Van Doren, M., Newman, S., Lehmann, R., 1998. zfh-1 is required for germ cell migration and gonadal mesoderm development in Drosophila. Development (Cambridge, England) 125, 655-666.

Brookman, J., Toosy, A., Shashidhara, L., White, R., 1992. The 412 retrotransposon and the development of gonadal mesoderm in Drosophila. Development (Cambridge, England) 116, 1185-1192.

Buescher, M., Svendsen, P.C., Tio, M., Miskolczi-McCallum, C., Tear, G., Brook, W.J., Chia, W., 2004. Drosophila T box proteins break the symmetry of hedgehog-dependent activation of wingless. Current biology : CB 14, 1694-1702.

Buescher, M., Tio, M., Tear, G., Overton, P., Brook, W., Chia, W., 2006. Functions of the segment polarity genes midline and H15 in Drosophila melanogaster neurogenesis. Developmental Biology 292, 418-429.

Cavarec, L., Jensen, S., Casella, J., Cristescu, S., Heidmann, T., 1997. Molecular cloning and characterization of a transcription factor for the copia retrotransposon with homology to the BTB-containing lola neurogenic factor. Molecular and cellular biology 17, 482-494.

Crowner, D., Madden, K., Goeke, S., Giniger, E., 2002. Lola regulates midline crossing of CNS axons in Drosophila. Development 129, 1317-1325.

Davies, E., Lim, J., Joo, W., Tam, C., Fuller, M., 2013. The transcriptional regulator lola is required for stem cell maintenance and germ cell differentiation in the Drosophila testis. Developmental Biology 373, 310-321.

DeFalco, T.J., Verney, G., Jenkins, A.B., McCaffery, J.M., Russell, S., Van Doren, M., 2003. Sex-specific apoptosis regulates sexual dimorphism in the Drosophila embryonic gonad. Dev Cell 5, 205-216.

Fairall, L., Schwabe, J.W., Chapman, L., Finch, J.T., Rhodes, D., 1993. The crystal structure of a two zinc-finger peptide reveals an extension to the rules for zinc-finger/DNA recognition. Nature 366, 483-487.

Formaz-Preston, A., Ryu, J.R., Svendsen, P.C., Brook, W.J., 2012. The Tbx20 homolog Midline represses wingless in conjunction with Groucho during the maintenance of segment polarity. Developmental Biology 369, 319-329.

Giniger, E., Tietje, K., Jan, L., Jan, Y., 1994. lola encodes a putative transcription factor required for axon growth and guidance in Drosophila. Development (Cambridge, England) 120, 1385-1398.

Goeke, S., Greene, E., Grant, P., Gates, M., Crowner, D., Aigaki, T., Giniger, E., 2003. Alternative splicing of lola generates 19 transcription factors controlling axon guidance in Drosophila. Nature neuroscience 6, 917-924.

Greig, S., Akam, M., 1995. The role of homeotic genes in the specification of the Drosophila gonad. Current biology : CB 5, 1057-1062.

Jemc, J., Milutinovich, A., Weyers, J., Takeda, Y., Van Doren, M., 2012. raw Functions through JNK signaling and cadherin-based adhesion to regulate Drosophila gonad morphogenesis. Developmental Biology 367, 114-125.

Jenkins, A., McCaffery, J., Van Doren, M., 2003. Drosophila E-cadherin is essential for proper germ cell-soma interaction during gonad morphogenesis. Development (Cambridge, England) 130, 4417-4426.

Kitadate, Y., Kobayashi, S., 2010. Notch and Egfr signaling act antagonistically to regulate germ-line stem cell niche formation in Drosophila male embryonic gonads. Proceedings of the National Academy of Sciences of the United States of America 107, 14241-14246.

Leal, S.M., Qian, L., Lacin, H., Bodmer, R., Skeath, J.B., 2009. Neuromancer1 and Neuromancer2 regulate cell fate specification in the developing embryonic CNS of Drosophila melanogaster. Developmental Biology 325, 138-150.

Lecuyer, E., Parthasarathy, N., Krause, H.M., 2008. Fluorescent in situ hybridization protocols in Drosophila embryos and tissues. Methods in molecular biology 420, 289-302.

Li, M., Alls, J., Avancini, R., Koo, K., Godt, D., 2003. The large Maf factor Traffic Jam controls gonad morphogenesis in Drosophila. Nature cell biology 5, 994-1000.

Liu, Q.-X., Hiramoto, M., Ueda, H., Gojobori, T., Hiromi, Y., Hirose, S., 2009. Midline governs axon pathfinding by coordinating expression of two major guidance systems. Genes & Development 23, 1165-1170.

Madden, K., Crowner, D., Giniger, E., 1999. LOLA has the properties of a master regulator of axon-target interaction for SNb motor axons of Drosophila. Developmental Biology 213, 301-313.

Mathews, W., Ong, D., Milutinovich, A., Van Doren, M., 2006. Zinc transport activity of Fear of Intimacy is essential for proper gonad morphogenesis and DE-cadherin expression. Development (Cambridge, England) 133, 1143-1153.

Miskolczi-McCallum, C., Scavetta, R., Svendsen, P., Soanes, K., Brook, W., 2005. The Drosophila melanogaster T-box genes midline and H15 are conserved regulators of heart development. Developmental Biology 278, 459-472.

Najand, N., Ryu, J.-R., Brook, W., 2012. In Vitro Site Selection of a Consensus Binding Site for the Drosophila melanogaster Tbx20 Homolog Midline. PLoS ONE 7.

Nusslein-Volhard, C., Wieschaus, E., Kluding, H., 1984. Mutations affecting the pattern of the larval cuticle in Drosophila melanogaster. Roux's Archives of Developmental Biology 193, 267-282.

Ohsako, T., Horiuchi, T., Matsuo, T., Komaya, S., Aigaki, T., 2003. Drosophila lola encodes a family of BTB-transcription regulators with highly variable C-terminal domains containing zinc finger motifs. Gene 311, 59-69.

Paige Bass, B., Cullen, K., McCall, K., 2007. The axon guidance gene lola is required for programmed cell death in the Drosophila ovary. Developmental Biology 304, 771-785.

Qian, L., Liu, J., Bodmer, R., 2005. Neuromancer Tbx20-related genes (H15/midline) promote cell fate specification and morphogenesis of the Drosophila heart. Developmental Biology 279, 509-524.

Reim, I., Frasch, M., 2005. The Dorsocross T-box genes are key components of the regulatory network controlling early cardiogenesis in Drosophila. Development 132, 4911-4925.

Reim, I., Mohler, J., Frasch, M., 2005. Tbx20-related genes, mid and H15, are required for tinman expression, proper patterning, and normal differentiation of cardioblasts in Drosophila. Mechanisms of development 122, 1056-1069.

Richardson, B., Lehmann, R., 2010. Mechanisms guiding primordial germ cell migration: strategies from different organisms. Nature reviews. Molecular cell biology 11, 37-49.

Riechmann, V., Rehorn, K.P., Reuter, R., Leptin, M., 1998. The genetic control of the distinction between fat body and gonadal mesoderm in Drosophila. Development 125, 713-723.

Ryu, J.-R., Najand, N., Brook, W., 2011. Tinman is a direct activator of midline in the Drosophila dorsal vessel. Developmental dynamics : an official publication of the American Association of Anatomists 240, 86-95.

Sano, H., Kunwar, P.S., Renault, A.D., Barbosa, V., Clark, I.B., Ishihara, S., Sugimura, K., Lehmann, R., 2012. The Drosophila Actin Regulator ENABLED Regulates Cell Shape and Orientation during Gonad Morphogenesis. PLoS ONE 7, e52649.

Spletter, M., Liu, J., Liu, J., Su, H., Giniger, E., Komiyama, T., Quake, S., Luo, L., 2007. Lola regulates Drosophila olfactory projection neuron identity and targeting specificity. Neural Development 2, 14.

Van Doren, M., Williamson, A., Lehmann, R., 1998. Regulation of zygotic gene expression in Drosophila primordial germ cells. Current biology : CB 8, 243-246.

Weyers, J., Milutinovich, A., Takeda, Y., Jemc, J., Van Doren, M., 2011. A genetic screen for mutations affecting gonad formation in Drosophila reveals a role for the slit/robo pathway. Developmental Biology 353, 217-228.

Yin, Z., Xu, X.L., Frasch, M., 1997. Regulation of the twist target gene tinman by modular cis-regulatory elements during early mesoderm development. Development 124, 4971-4982.

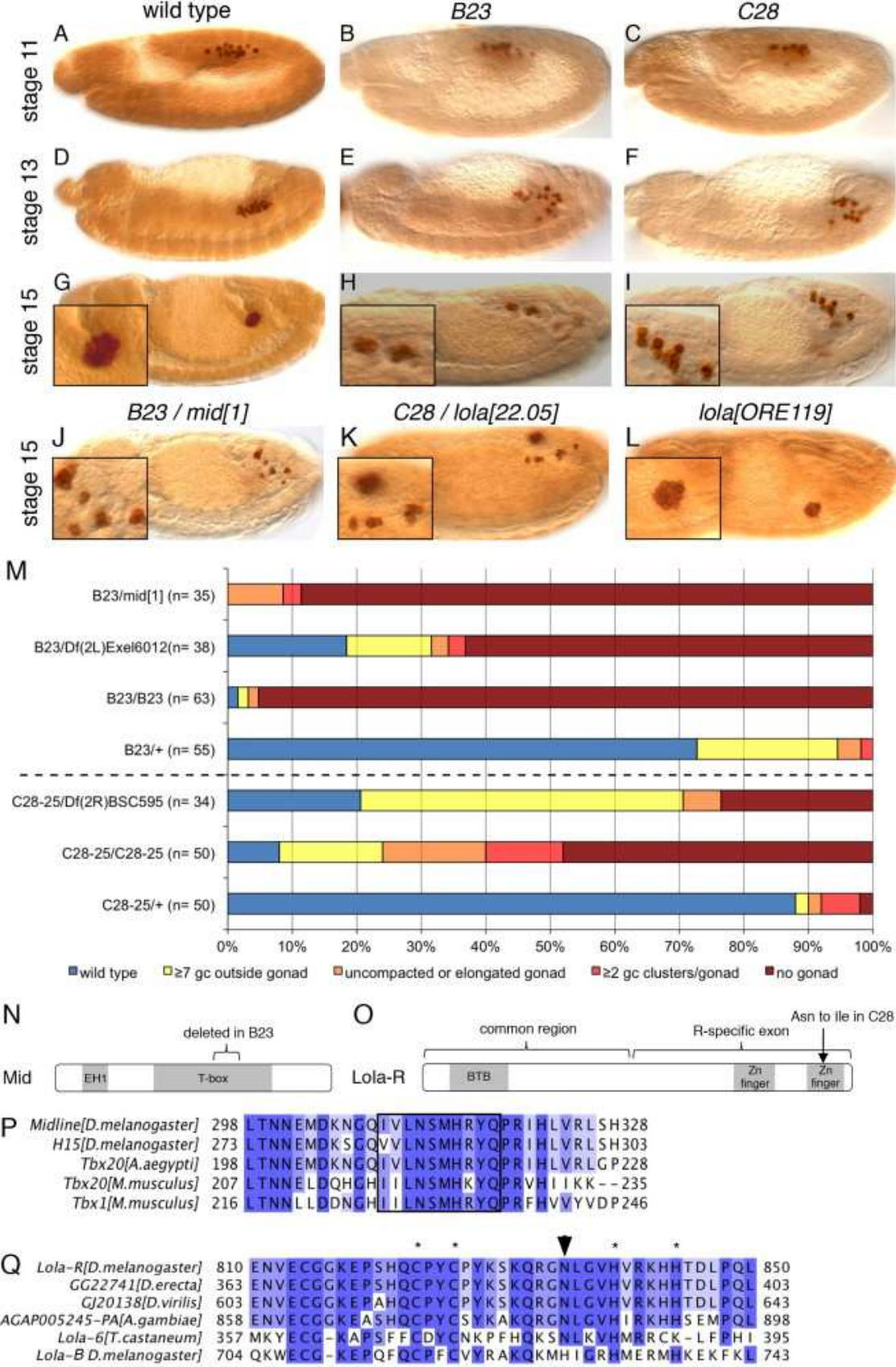
wild type
B23
C28
stage 11
stage 13
stage 15
stage 15
A
B
C
D
E
F
G
H
I
J
K
L
B23 / mid[1]
C28 / lola[22.05]
lola[ORE119]
M
B23/mid[1] (n= 35)
B23/Df(2L)Exel6012(n= 38)
B23/B23 (n= 63)
B23/+ (n= 55)
C28-25/Df(2R)BSC595 (n= 34)
C28-25/C28-25 (n= 50)
C28-25/+ (n= 50)
0%
10%
20%
30%
40%
50%
60%
70%
80%
90%
100%
wild type
≥7 gc outside gonad
uncompacted or elongated gonad
≥2 gc clusters/gonad
no gonad
N
deleted in B23
Mid
EH1
T-box
O
common region
R-specific exon
Asn to Ile in C28
Lola-R
BTB
Zn finger
Zn finger
P
Midline[D.melanogaster] 298 LTNNEMDKNGQIVLNSMHRYQPRIHLVRLSH328
H15[D.melanogaster] 273 LTNNEMDKSGQVVLNSMHRYQPRIHLVRLSH303
Tbx20[A.aegypti] 198 LTNNEMDKNGQIVLNSMHRYQPRIHLVRLGP228
Tbx20[M.musculus] 207 LTNNELDQHGHIILNSMHKYQPRVHIIKK--235
Tbx1[M.musculus] 216 LTNNLLDDNGHIILNSMHRYQPRFHVVYVDP246
Q
Lola-R[D.melanogaster] 810 ENVECGGKEPSHQCPYCPYKSKQRGNLGVHVRKHHTDLPQL 850
GG22741[D.erecta] 363 ENVECGGKEPSHQCPYCPYKSKQRGNLGVHVRKHHTDLPQL 403
GJ20138[D.virilis] 603 ENVECGGKEPAHQCPYCPYKSKQRGNLGVHVRKHHTDLPQL 643
AGAP005245-PA[A.gambiae] 858 ENVECGGKEASHQCPYCSYKAKQRGNLGVHIRKHHSEMPQL 898
Lola-6[T.castaneum] 357 MKYECG-KAPSFFCDYCNKPFHQKSNLKVHMRRCK-LFPHI 395
Lola-B D.melanogaster] 704 QKWECG-KEPQFQCPFCVYRAKQKMHIGRHMERMHKEKFKL 743

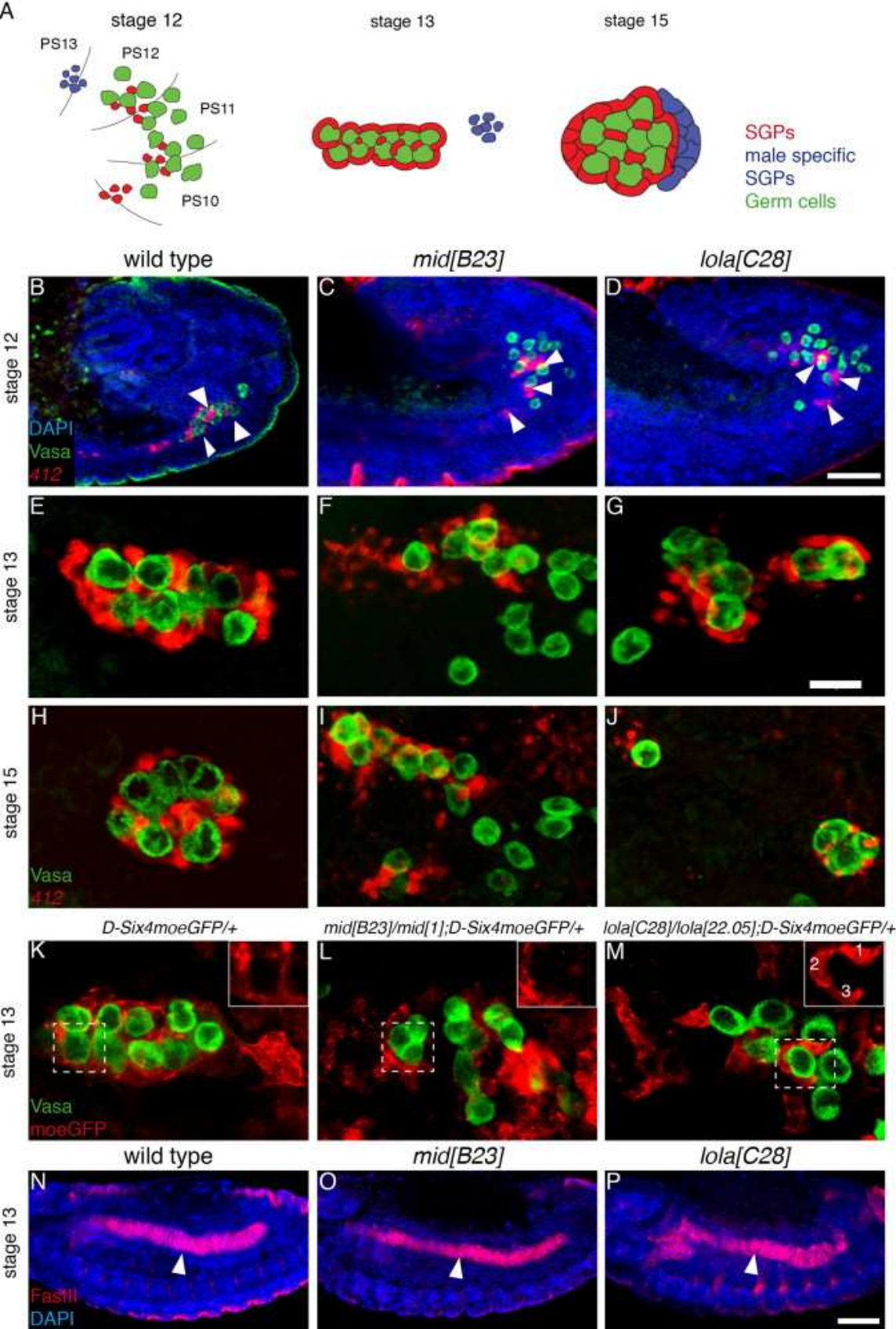
A
stage 12
stage 13
stage 15
PS13
PS12
PS11
PS10
SGPs
male specific SGPs
Germ cells
wild type
mid[B23]
lola[C28]
stage 12
stage 13
stage 15
B
C
D
E
F
G
H
I
J
DAPI
Vasa
412
D-Six4moeGFP/+
mid[B23]/mid[1];D-Six4moeGFP/+
lola[C28]/lola[22.05];D-Six4moeGFP/+
K
L
M
Vasa
moeGFP
1
2
3
wild type
mid[B23]
lola[C28]
N
O
P
FasIII
DAPI

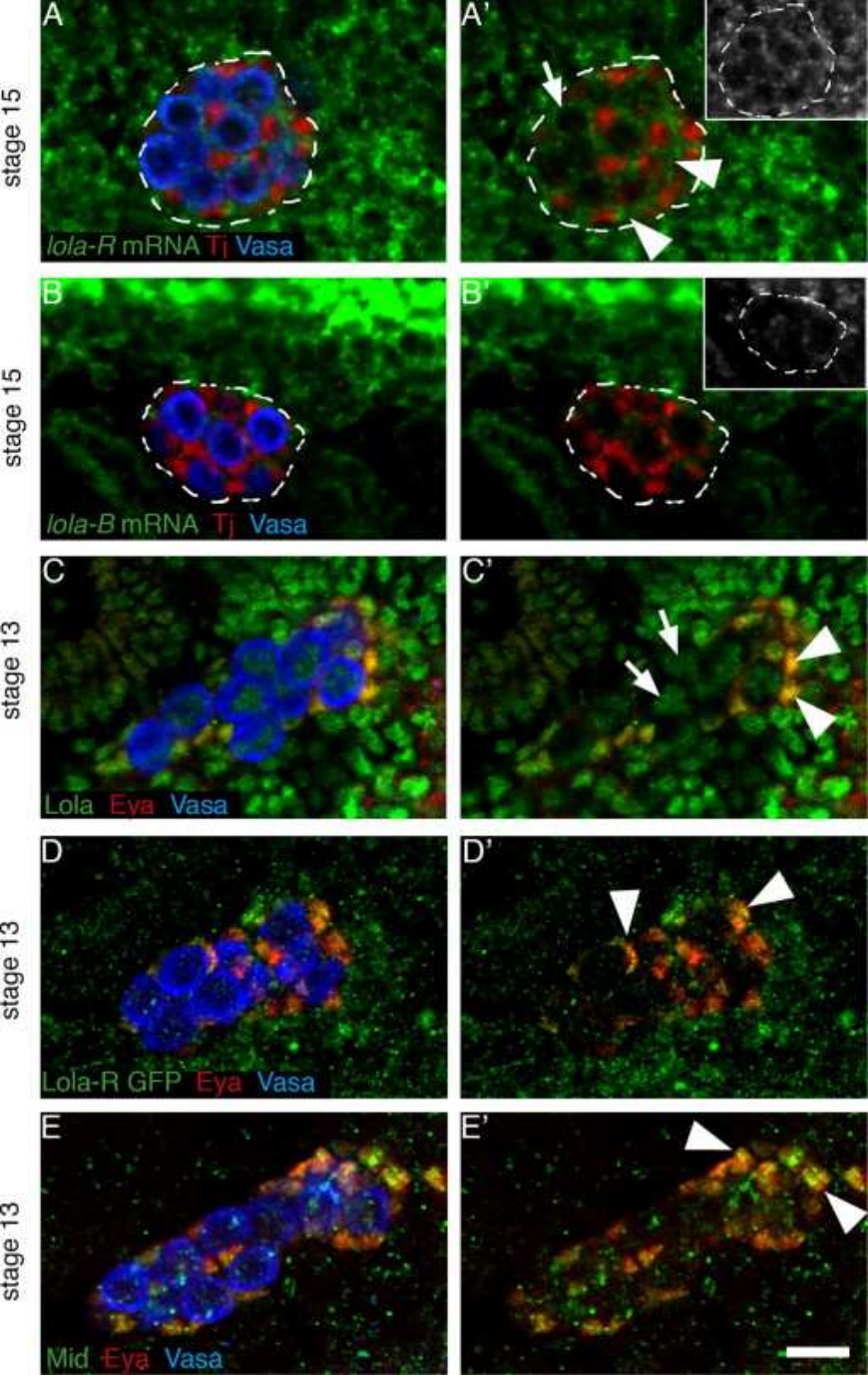
stage 15
A
A'
lola-R mRNA Tj Vasa
stage 15
B
B'
lola-B mRNA Tj Vasa
stage 13
C
C'
Lola Eya Vasa
stage 13
D
D'
Lola-R GFP Eya Vasa
stage 13
E
E'
Mid Eya Vasa

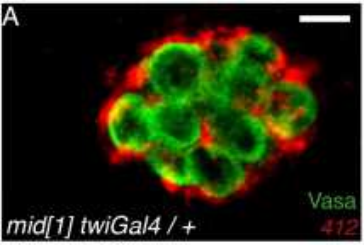
A
Vasa
412
mid[1] twiGal4 / +

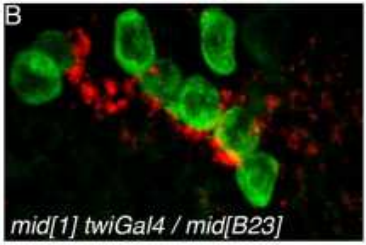
B
mid[1] twiGal4 / mid[B23]

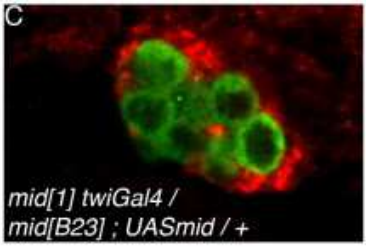
C
mid[1] twiGal4 /
mid[B23] ; UASmid / +

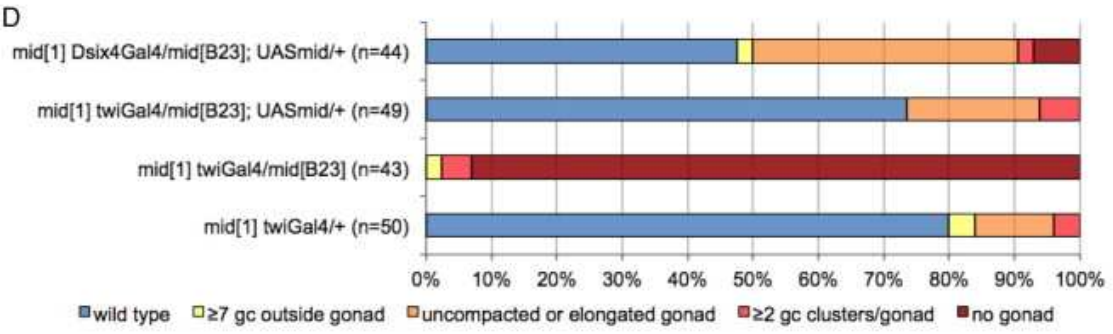
D
mid[1] Dsix4Gal4/mid[B23]; UASmid/+ (n=44)
mid[1] twiGal4/mid[B23]; UASmid/+ (n=49)
mid[1] twiGal4/mid[B23] (n=43)
mid[1] twiGal4/+ (n=50)
0%
10%
20%
30%
40%
50%
60%
70%
80%
90%
100%
wild type
≥7 gc outside gonad
uncompacted or elongated gonad
≥2 gc clusters/gonad
no gonad

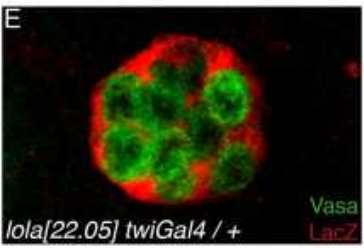
E
Vasa
LacZ
lola[22.05] twiGal4 / +

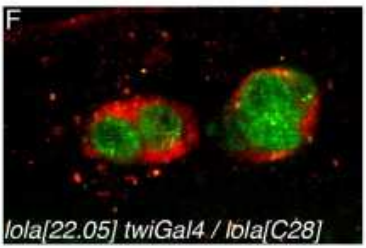
F
lola[22.05] twiGal4 / lola[C28]

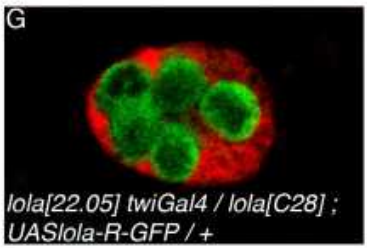
G
lola[22.05] twiGal4 / lola[C28] ;
UASlola-R-GFP / +

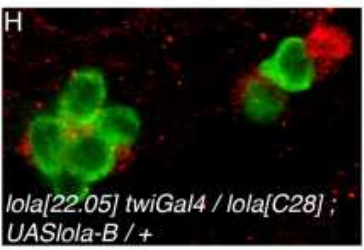
H
lola[22.05] twiGal4 / lola[C28] ;
UASlola-B / +

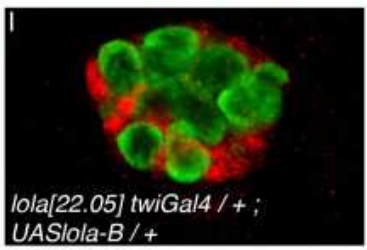
I
lola[22.05] twiGal4 / + ;
UASlola-B / +

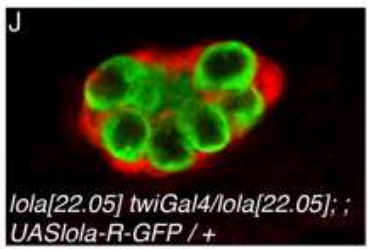
J
lola[22.05] twiGal4/lola[22.05]; ;
UASlola-R-GFP / +

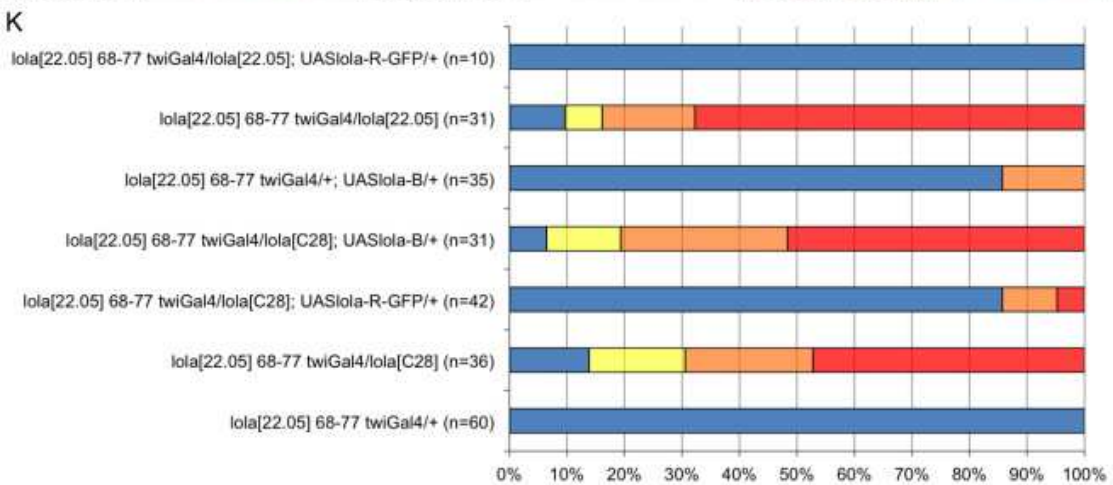
K
lola[22.05] 68-77 twiGal4/lola[22.05]; UASlola-R-GFP/+ (n=10)
lola[22.05] 68-77 twiGal4/lola[22.05] (n=31)
lola[22.05] 68-77 twiGal4/+; UASlola-B/+ (n=35)
lola[22.05] 68-77 twiGal4/lola[C28]; UASlola-B/+ (n=31)
lola[22.05] 68-77 twiGal4/lola[C28]; UASlola-R-GFP/+ (n=42)
lola[22.05] 68-77 twiGal4/lola[C28] (n=36)
lola[22.05] 68-77 twiGal4/+ (n=60)
0%
10%
20%
30%
40%
50%
60%
70%
80%
90%
100%
wild type gonad
≥7 gc outside gonad
uncompacted or elongated gonad
≥2 SGP clusters/gonad

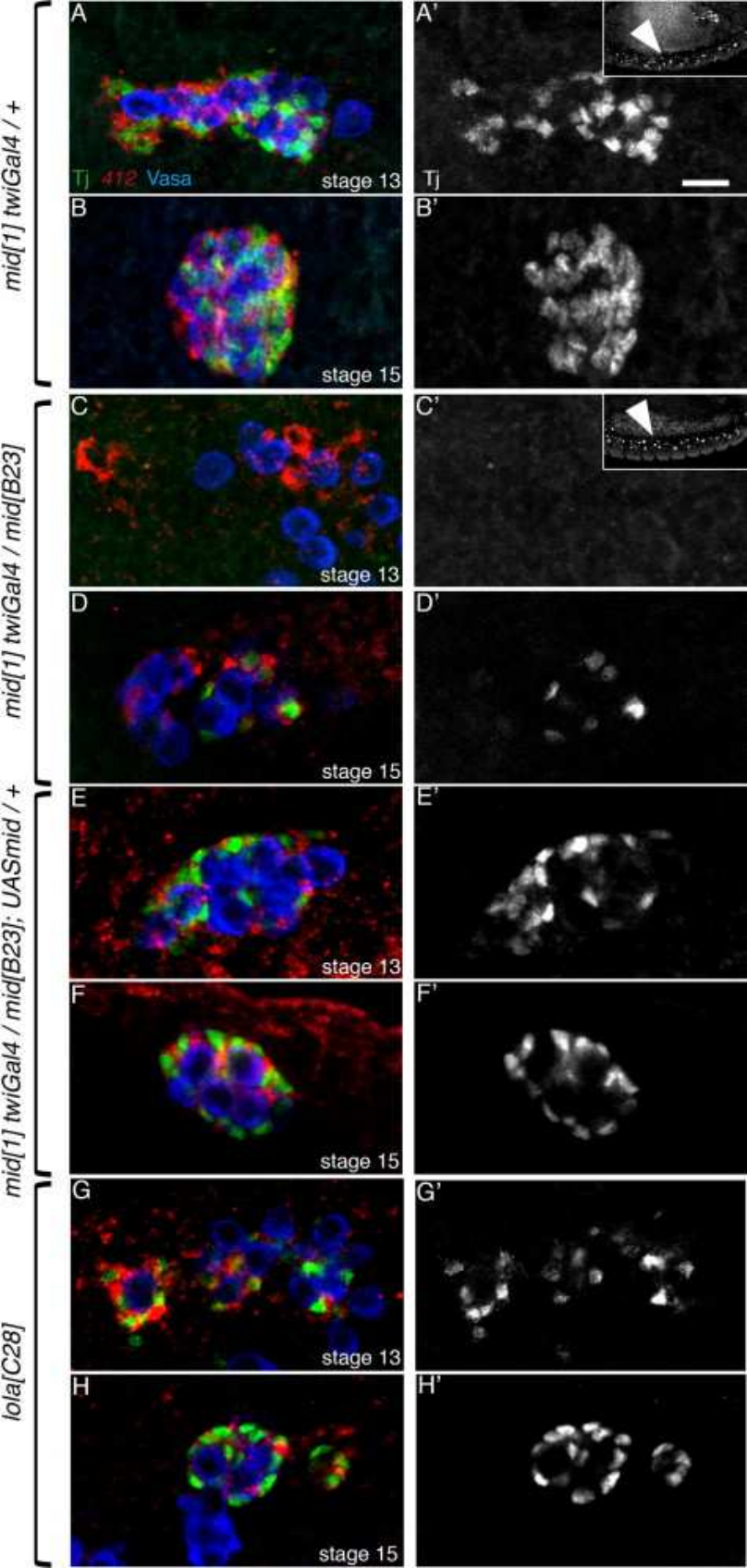
mid[1] twiGal4 / +
mid[1] twiGal4 / mid[B23]
mid[1] twiGal4 / mid[B23]; UASmid / +
lola[C28]
A
Tj 412 Vasa
stage 13
A'
Tj
B
stage 15
B'
C
stage 13
C'
D
stage 15
D'
E
stage 13
E'
F
stage 15
F'
G
stage 13
G'
H
stage 15
H'

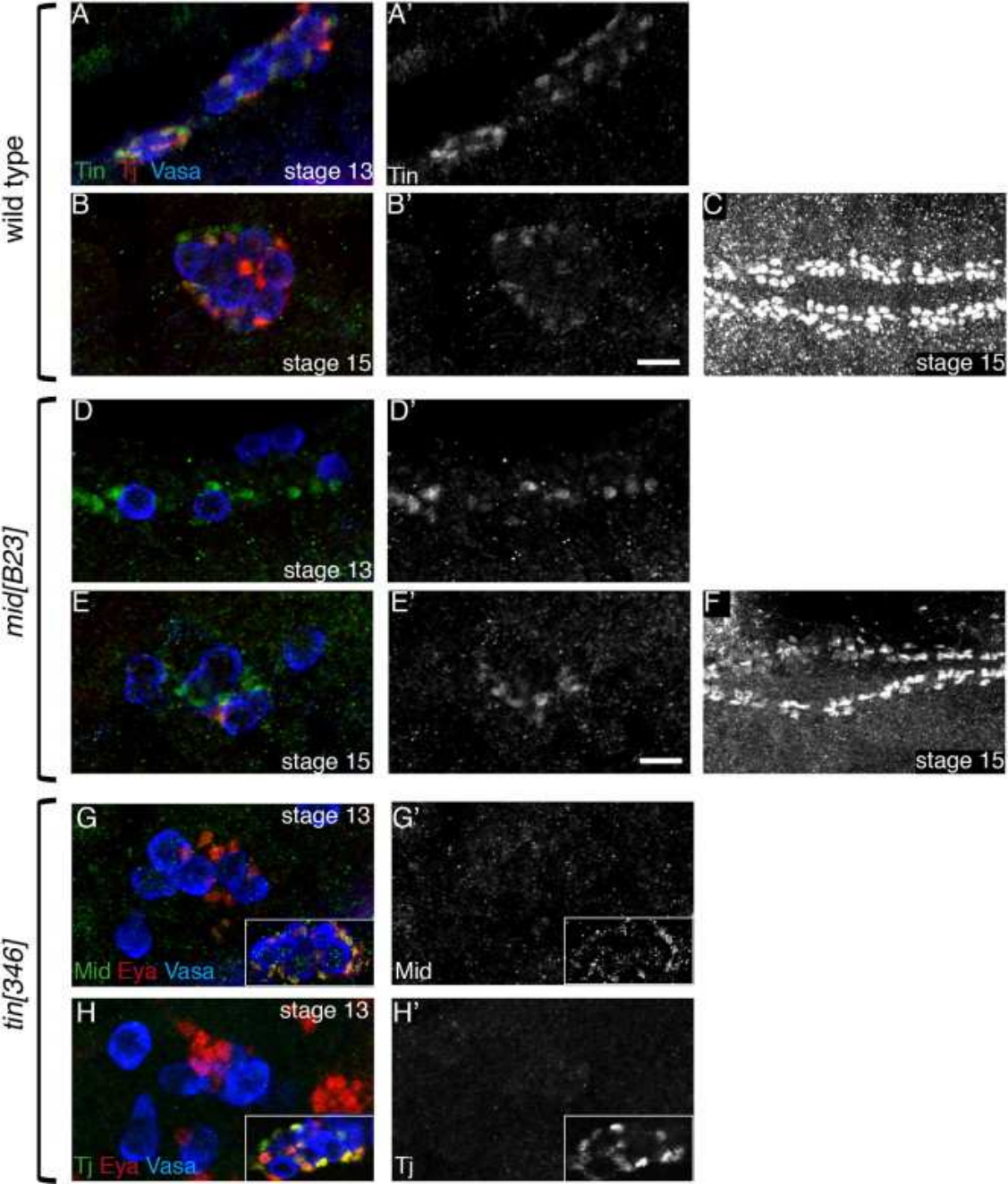
wild type
A
Tin Tj Vasa
stage 13
A'
Tin
B
stage 15
B'
C
stage 15
mid[B23]
D
stage 13
D'
E
stage 15
E'
F
stage 15
tin[346]
G
stage 13
Mid Eya Vasa
G'
Mid
H
stage 13
Tj Eya Vasa
H'
Tj

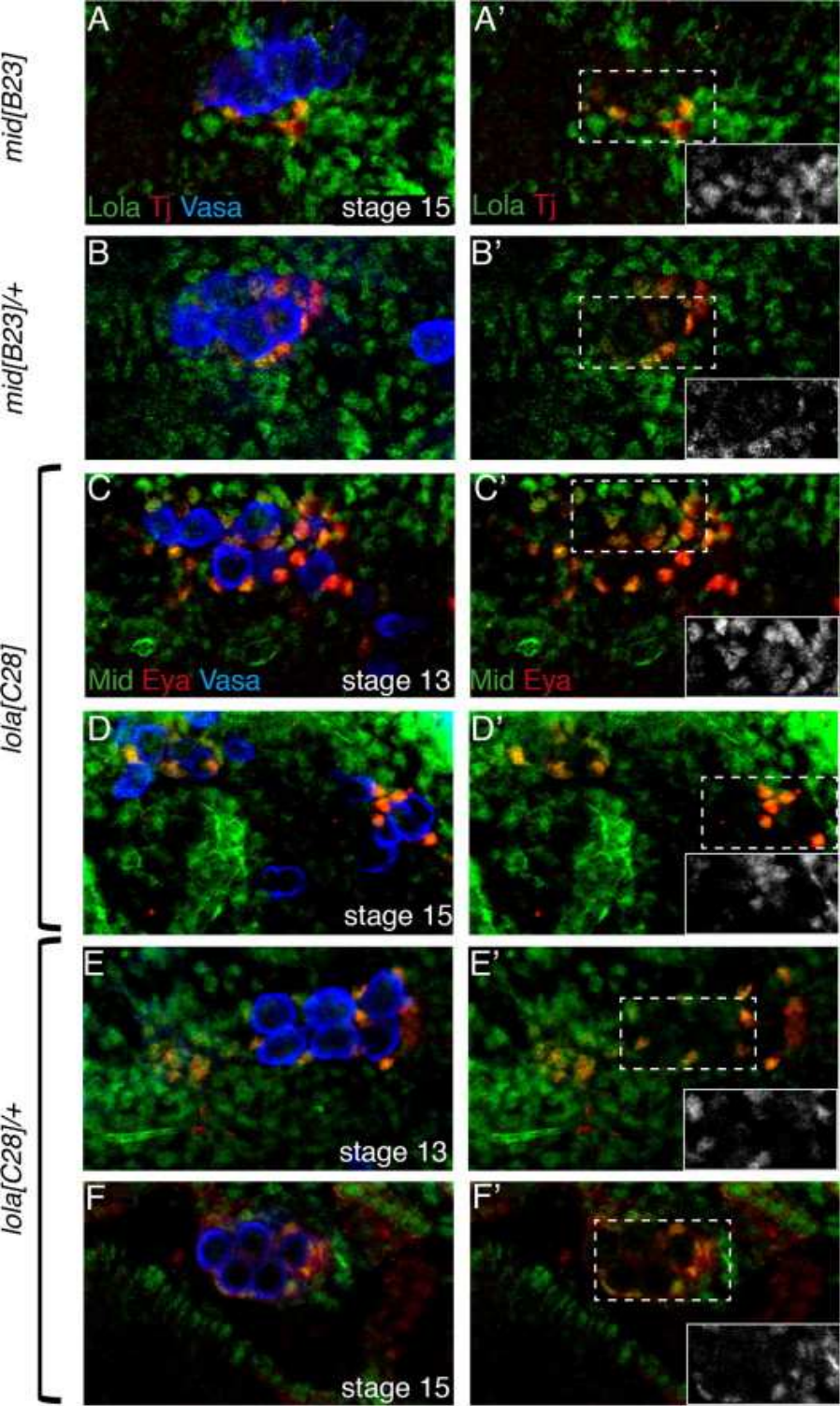
mid[B23]
mid[B23]/+
lola[C28]
lola[C28]/+
A
A'
Lola Tj Vasa
stage 15
Lola Tj
B
B'
C
C'
Mid Eya Vasa
stage 13
Mid Eya
D
D'
stage 15
E
E'
stage 13
F
F'
stage 15

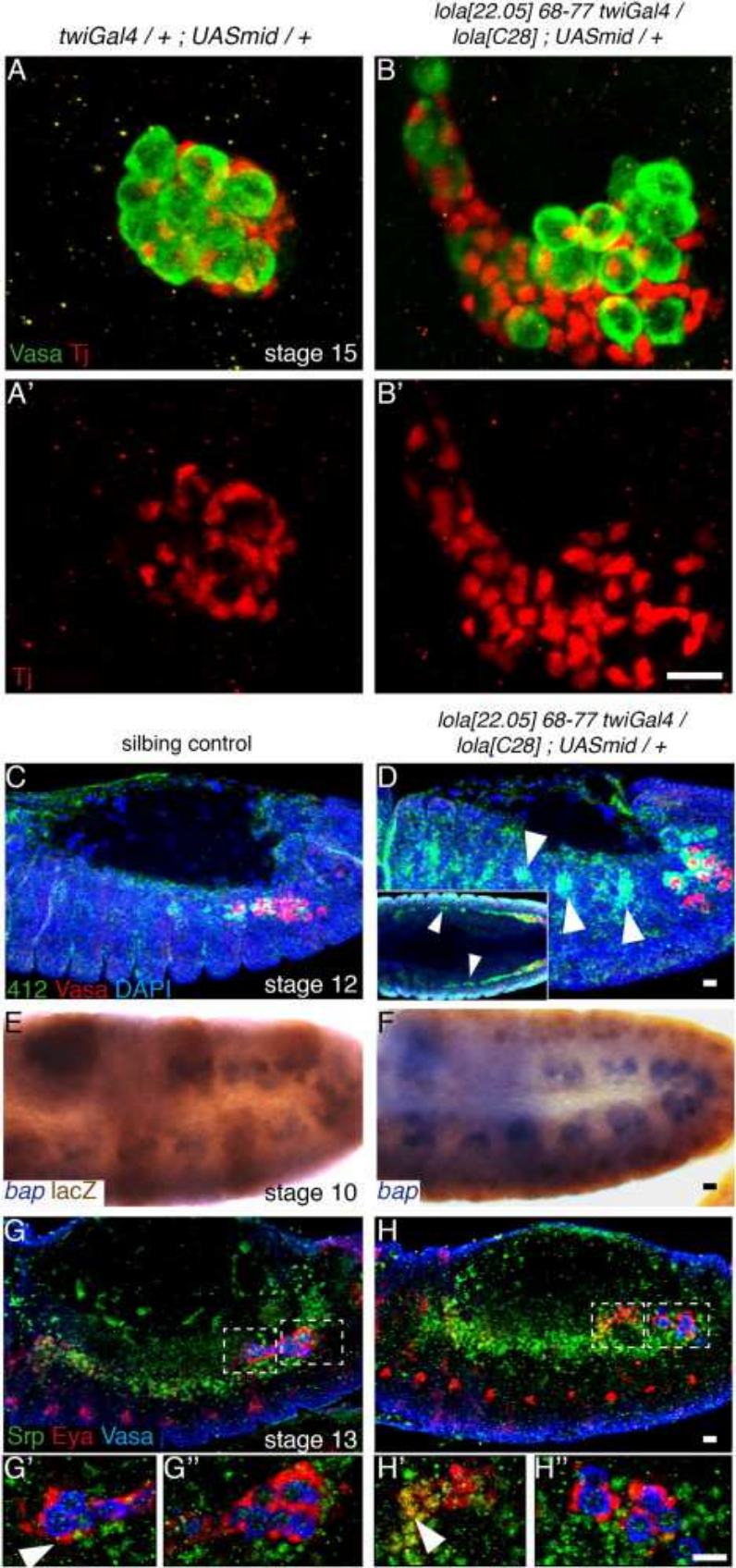
twiGal4 / + ; UASmid / +
lola[22.05] 68-77 twiGal4 /
lola[C28] ; UASmid / +
A
B
Vasa Tj
stage 15
A'
B'
Tj
silbing control
lola[22.05] 68-77 twiGal4 /
lola[C28] ; UASmid / +
C
D
412 Vasa DAPI
stage 12
E
F
bap lacZ
stage 10
bap
G
H
Srp Eya Vasa
stage 13
G'
G''
H'
H''

Figure S1

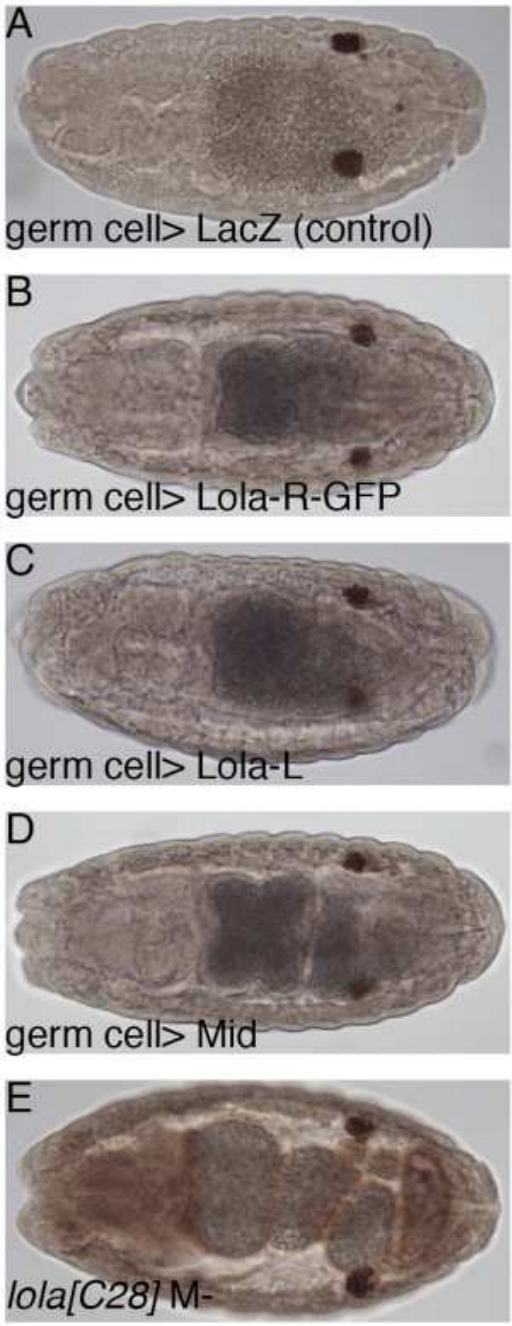
A
germ cell> LacZ (control)
B
germ cell> Lola-R-GFP
C
germ cell> Lola-L
D
germ cell> Mid
E
lola[C28] M-

Fig S2

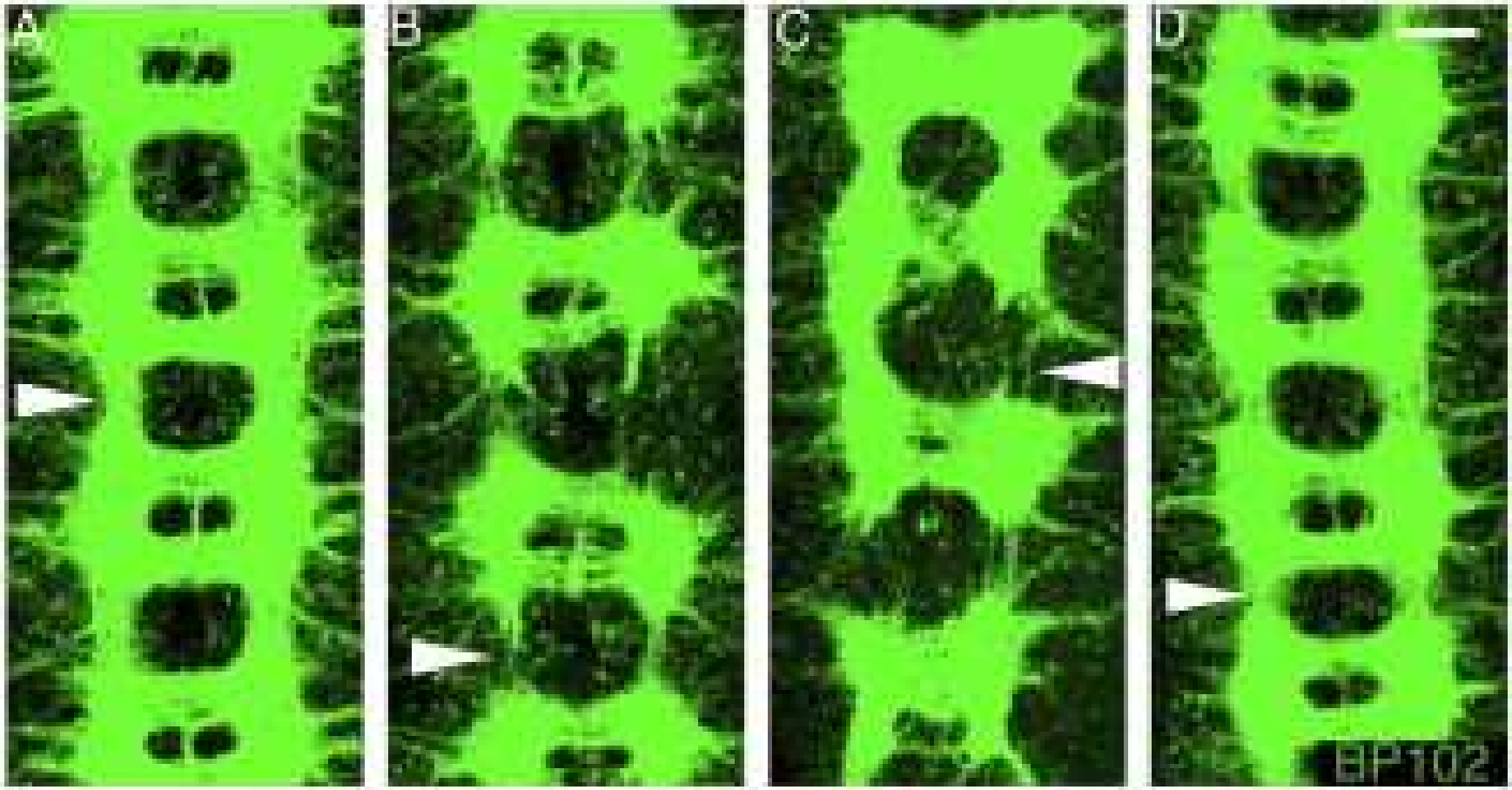

wild type *mld[B23]* *lola[22.05]* *lola[C28]*

Fig S3

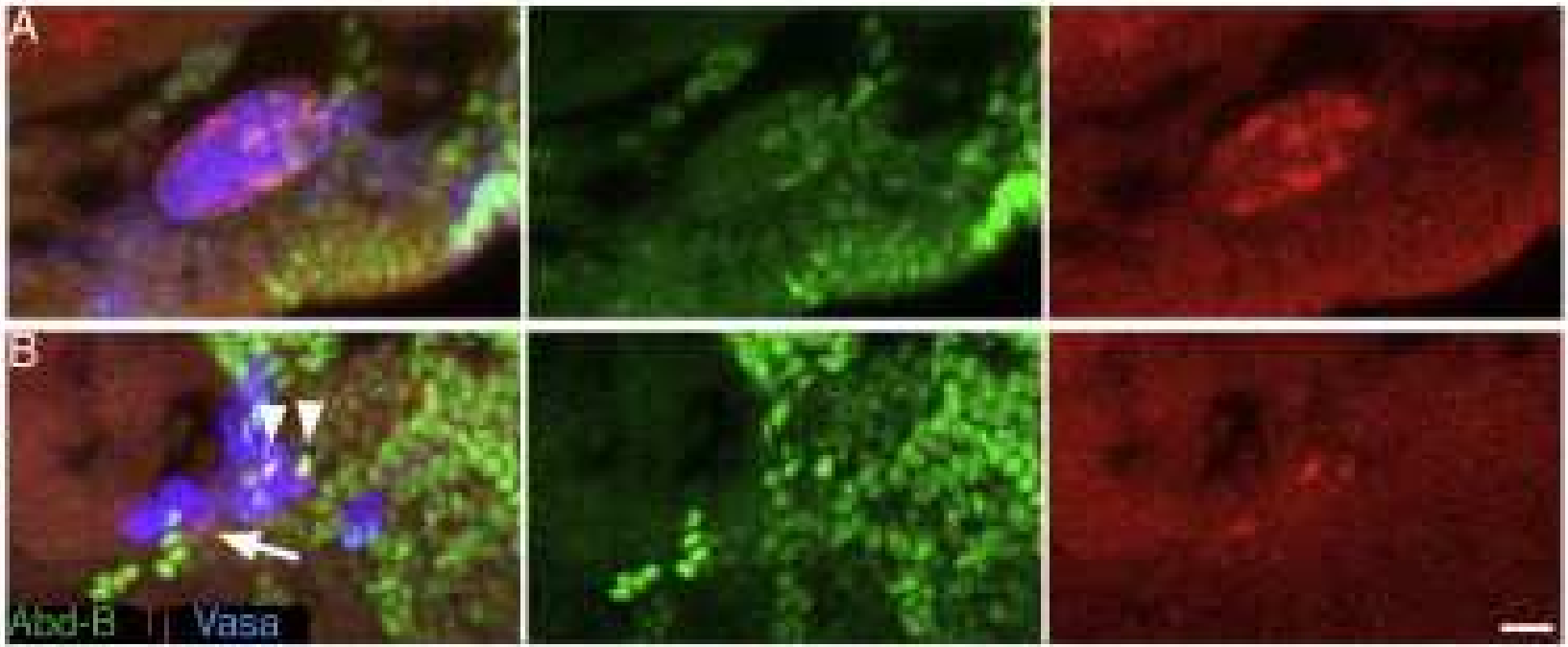

Fig S4

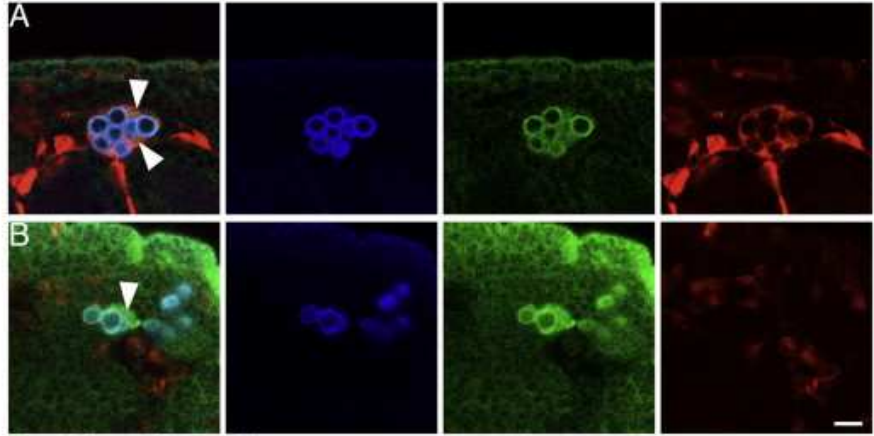

Fig S5

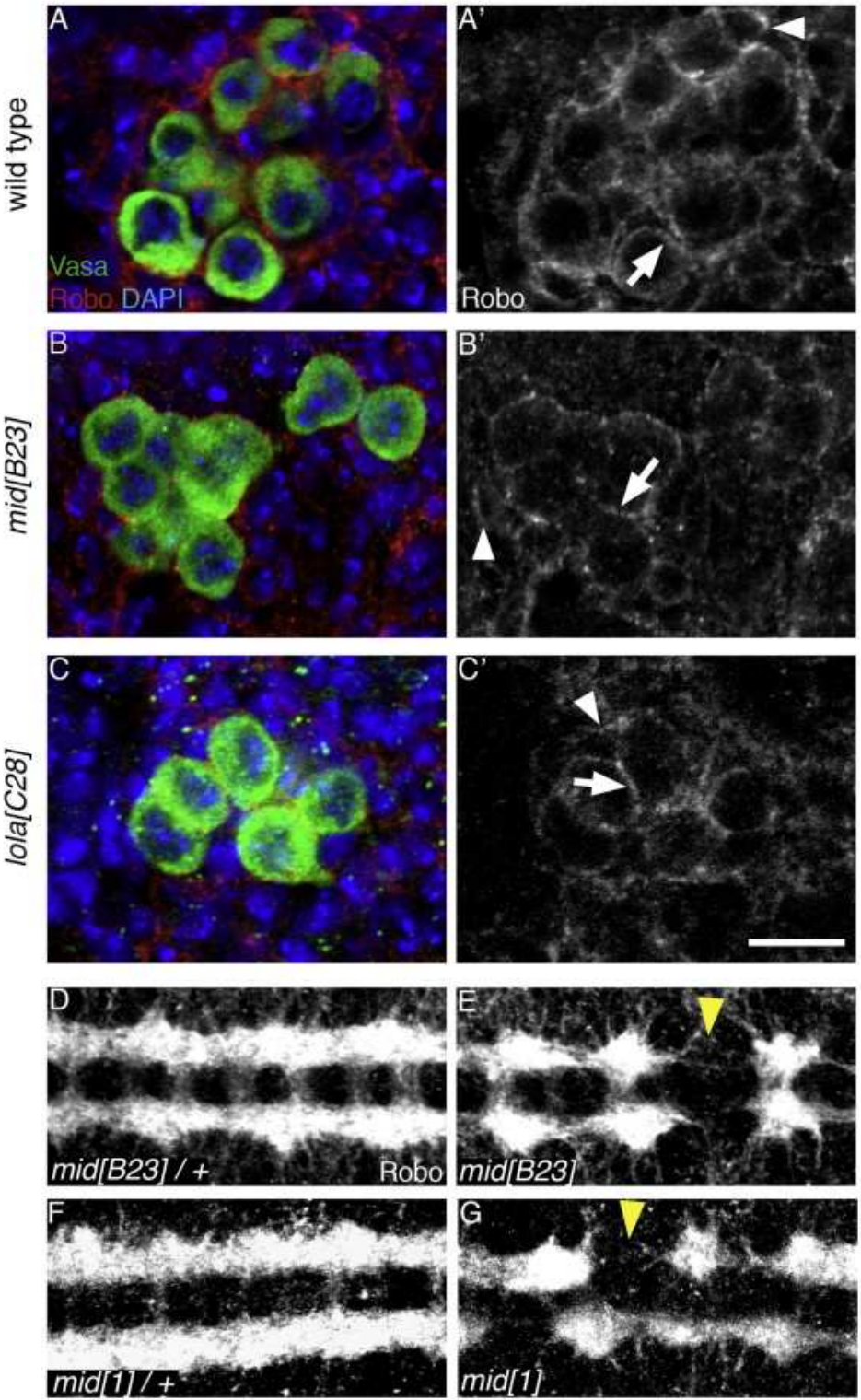
wild type
mid[B23]
lola[C28]
A
A'
Vasa
Robo DAPI
Robo
B
B'
C
C'
D
E
mid[B23] / +
Robo
mid[B23]
F
G
mid[1] / +
mid[1]

Fig S6

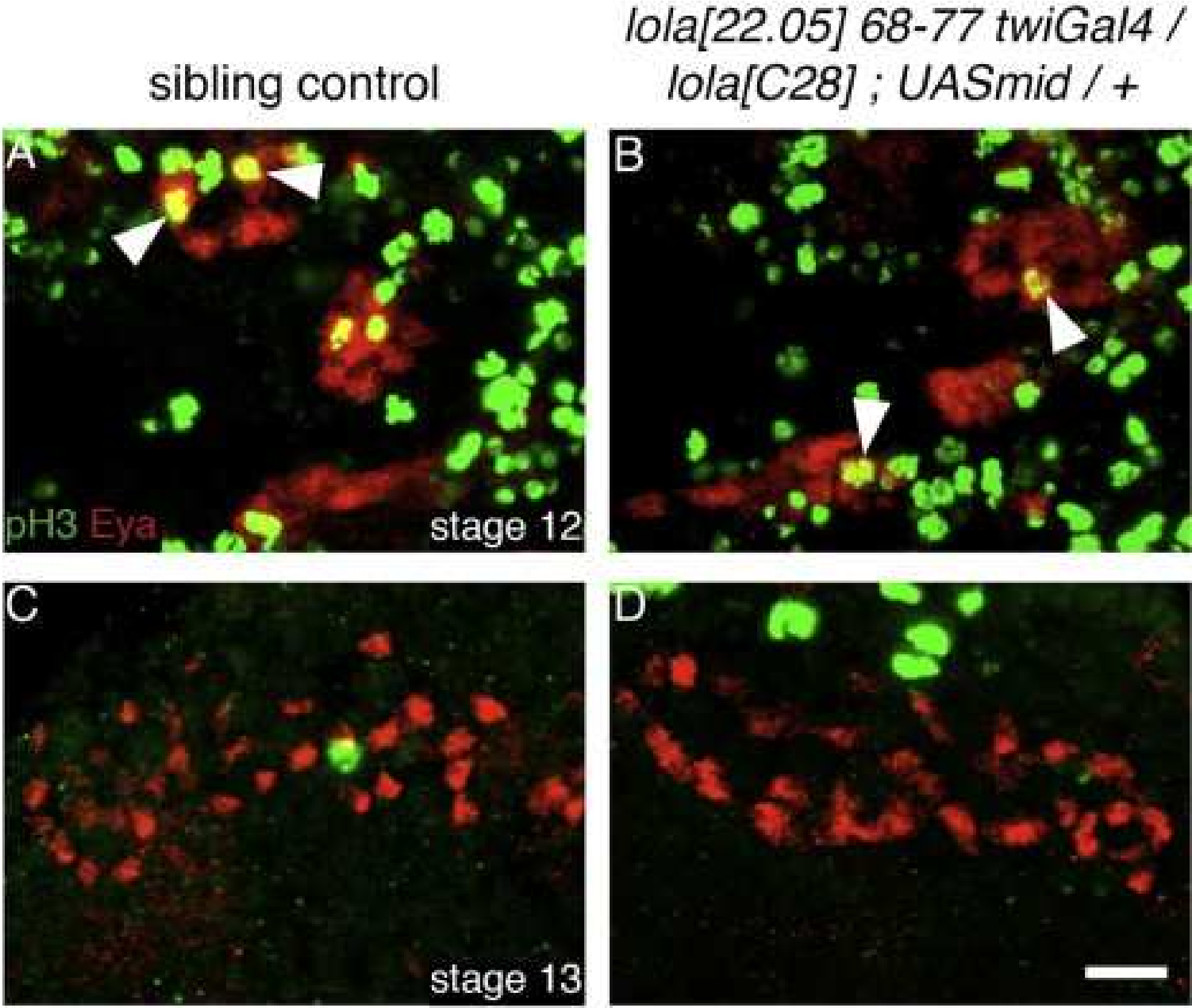
sibling control
lola[22.05] 68-77 twiGal4 /
lola[C28] ; UASmid / +
A
B
pH3 Eya
stage 12
C
D
stage 13